ISTANBUL TECHNICAL UNIVERSITY ★ GRADUATE SCHOOL

CYCLODEXTRIN-FUNCTIONAL NANOFIBERS AS HORMONE DELIVERY SYSTEMS

M.Sc. THESIS

Mohamad Yamen KET

Department of Chemistry

Chemistry Programme

JANUARY 2025

ISTANBUL TECHNICAL UNIVERSITY ★ GRADUATE SCHOOL

CYCLODEXTRIN-FUNCTIONAL NANOFIBERS AS HORMONE DELIVERY SYSTEMS

M.Sc. THESIS

Mohamad Yamen KET
(509201218)

Department of Chemistry

Chemistry Programme

Thesis Advisor: Assoc. Prof. Dr. Fuat TOPUZ

JANUARY 2025

ISTANBUL TEKNİK ÜNİVERSİTESİ ★ LİSANSÜSTÜ EĞİTİM ENSTİTÜSÜ

SİKLODEKSTRİN FONKSİYONLU NANOLİFLERİN HORMON SALIM SİSTEMLERİ OLARAK KULLANIMLARI

YÜKSEK LİSANS TEZİ

Mohamad Yamen KET
(509201218)

Kimya Anabilim Dalı

Kimya Programı

Tez Danışmanı: Doç. Dr. Fuat TOPUZ

OCAK 2025

Mohamad Yamen Ket, a M.Sc. student of İTU Graduate School student ID 509201218 successfully defended the thesis/dissertation entitled "CYCLODEXTRIN-FUNCTIONAL NANOFIBERS AS HORMONE DELIVERY SYSTEMS", which he prepared after fulfilling the requirements specified in the associated legislations, before the jury whose signatures are below.

Thesis Advisor :	**Assoc. Prof. Dr. Fuat TOPUZ** Istanbul Technical University	.....
Jury Members :	**Asst. Prof. Dr. Berkay SÜTAY** Istanbul Technical University	.....
	Asst. Prof. Dr. Yelda BİRİNCİ KUDU Istinye University	.....

Date of Submission : 10 January 2025
Date of Defense : 17 February 2025

FOREWORD

I dedicate this thesis to the soul of my beloved father, Hussien, my dear mum and siblings, Ali, Hossam, and Bana. I couldn't do it without their support and encouragement.

My dear friends, Wissem Mhiri, who helped me apply to this program and Saeed Zaineddin, who were more than a brother to me here in Istanbul.

Büşra Kayıkçı, whose beautiful music uplifted my spirit and helped me focus throughout this journey.

My academic advisor, Assoc. Prof. Dr. Fuat Topuz, for your guidance, wisdom, and patience. You have been more than a teacher for me, and I cannot thank you enough for all the help you have given me.

And to every friend who supported me in one way or another throughout my academic journey.

I would like to express my sincere gratitude to Asst. Prof. Dr. Berkay Sütay and Asst. Prof. Dr. Yelda Birinci Kudu for serving as members of my thesis jury and for their valuable comments and suggestions.

January 2025

Mohamad Yamen KET
(Chemist)

TABLE OF CONTENTS

Page

ABBREVIATIONS

AcOH	**:** Acetic acid
CA	**:** Cellulose acetate
CD	**:** Cyclodextrin
E2	**:** Estradiol
E3	**:** Estriol
FTIR	**:** Fourier transform infrared spectroscopy
Gel	**:** Gelatin
HP-β-CD	**:** Hydroxypropyl-beta-cyclodextrin
HP-γ-CD	**:** Hydroxypropyl-gamma-cyclodextrin
IC	**:** Inclusion complex
Mw	**:** Molecular weight
NF	**:** Nanofibers
P4	**:** Progesterone
Pul	**:** Pullulan
SEM	**:** Scanning electron microscopy
TGA	**:** Thermogravimetric analysis
UV-Vis	: Ultraviolet visible spectroscopy
V	**:** Volume
% (w/v)	**:** Weight/volume percentage
% (w/w)	**:** Weight/weight percentage

LIST OF TABLES

Page

LIST OF FIGURES

Page

CYCLODEXTRIN-FUNCTIONAL NANOFIBERS AS HORMONE DELIVERY SYSTEMS

SUMMARY

This thesis focuses on the development of cyclodextrin (CD)-functionalized polymer nanofibers for use in hormone delivery systems. Particular emphasis is placed on the rational selection of hydrophilic and hydrophobic polymers, the incorporation of hormones at varying concentrations, and the role of CD inclusion in modulating drug loading capacity, drug stability, and release kinetics. The study evaluates the release behavior of hormone-loaded nanofibers, with the aim of achieving both rapid and sustained release profiles. Hydrophilic polymers such as pullulan and gelatin are utilized to achieve rapid drug release *via* fast-disintegrating fibers, while hydrophobic cellulose acetate (CA) is employed to promote sustained drug release. In each formulation, the incorporation of CDs enhances the solubility and stability of the hormones, while simultaneously modulating their release profiles from the nanofibrous structures.

Hormone delivery, especially oral administration of hormones such as progesterone (P4), estradiol (E2), and estriol (E3), presents significant therapeutic importance due to their central roles in regulating a wide range of physiological processes. These steroidal hormones, although endogenously produced, are frequently supplemented from external sources in clinical settings due to fluctuations, deficiencies, or dysfunctions in the body's natural hormone production. Their inclusion in this study is based on both their clinical relevance and their physicochemical challenges, such as poor aqueous solubility and instability, which complicate conventional oral delivery.

P4 is a crucial hormone involved in regulating the menstrual cycle, maintaining pregnancy, and supporting embryogenesis. It is primarily secreted by the corpus luteum and later by the placenta during pregnancy. P4 prepares the endometrium for embryo implantation and sustains early pregnancy. However, progesterone levels may be insufficient due to luteal phase defects, anovulation, or during hormone replacement therapy (HRT) for peri- and postmenopausal women. Supplementation of P4 is essential in assisted reproductive technologies (ART), luteal phase support, and the treatment of conditions such as endometrial hyperplasia.

E2, the most potent naturally occurring estrogen, is essential for reproductive health, maintaining bone density, cardiovascular protection, and neuroprotection. E2 levels significantly decline during menopause, leading to symptoms such as hot flashes, mood swings, and an increased risk of osteoporosis. Clinically, E2 is used in HRT for

menopausal women, treatment of hypogonadism, and managing estrogen deficiencies following surgical removal of ovaries or other medical conditions.

E3, while considered a weaker estrogen than E2, plays a vital role during pregnancy and is gaining recognition for its therapeutic potential due to its favorable safety profile. E3 is commonly used in HRT, particularly in women who cannot tolerate stronger estrogens. It exhibits tissue-selective activity with a lower risk of stimulating endometrial or breast tissue, making it a safer alternative for long-term use.

Despite the body's inherent ability to synthesize these hormones, external supplementation is often required to restore physiological levels, manage hormone-related disorders, or compensate for age- or disease-related decline in endogenous production. Additionally, when hormones are administered orally, they often undergo significant first-pass metabolism in the liver, drastically reducing their bioavailability. The result is not only lower systemic levels but also greater interindividual variability in response and increased metabolic byproducts, which can lead to side effects.

This thesis addresses these challenges by exploiting CD-functionalized nanofibers, which represent a novel approach to overcoming these obstacles. By combining the unique inclusion-complex-forming ability of CDs with the versatility of electrospinning, this work pioneers the development of advanced nanofiber systems capable of tailoring release profiles for both rapid and sustained delivery. The incorporation of hydrophilic and hydrophobic polymers in a single system further enhances the potential for personalized and efficient oral hormone therapy.

The thesis begins by introducing the fundamentals of electrospinning and its application in fabricating electrospun fibers for oral drug delivery. It then examines the electrospinning process of hormone-loaded, CD-functionalized polymer fibers and their potential in hormone delivery systems. This is followed by an experimental section that provides a detailed overview of the materials used and the conducted experiments.

The fourth chapter presents an investigation into the encapsulation and release behavior of the selected hormones— P4, E2, and E3—from hydrophilic electrospun pullulan-based fibers. These hormones, due to their hydrophobicity and poor aqueous solubility, were first complexed with CDs to improve their compatibility with the hydrophilic polymer matrix. The resulting inclusion complexes (ICs) were then incorporated into pullulan solutions and processed *via* electrospinning. Optimization of electrospinning parameters—such as polymer concentration, flow rate, voltage, and tip-to-collector distance—was carefully performed to obtain uniform, bead-free fibers. Fiber morphology was examined using optical microscopy and scanning electron microscopy (SEM), both of which confirmed the successful formation of continuous, smooth fibers with nanometer-scale diameters and no visible aggregates or crystalline hormone residues. The incorporation of hormone–CD complexes did not negatively affect fiber formation, indicating good compatibility between the drug complexes and the polymer matrix. FTIR analysis confirmed the successful encapsulation of P4, E2, and E3 within the fibers by identifying characteristic hormone peaks.

TGA results demonstrated enhanced thermal stability of the encapsulated hormones, evidenced by higher decomposition temperatures compared to raw drugs and CD complexes. *In vitro* release studies were carried out in aqueous media to evaluate the drug release kinetics of the pullulan-based systems. The hydrophilic nature of pullulan enabled rapid fiber disintegration upon contact with simulated saliva, resulting in an immediate burst release of the encapsulated hormones. This fast-release profile is particularly valuable for buccal or sublingual administration, where rapid absorption through the mucosal membranes is desired. The data confirmed that hormone release was achieved within minutes, making these systems ideal for applications requiring quick onset of action, such as hormone deficiency crises or short-term therapeutic interventions.

In the subsequent chapter, the thesis explores a more complex nanofiber design involving multilayered fibers with a sandwich structure to achieve controlled hormone release. This system consisted of hydrophobic CA as the outer layers and gelatin, a hydrophilic, biocompatible polymer, as the inner core layer. The inner gelatin layer contained the hormone–CD complexes, while the CA layers served as diffusion barriers to modulate the release rate. The fabrication of this multilayered structure was achieved through a sequential electrospinning process. Each layer was deposited with controlled thickness and alignment to ensure homogeneity and reproducibilityOptical microscopy was used to examine the fiber structure of each layer, while FTIR analysis verified the encapsulation of hormones at varying concentrations. Release studies demonstrated that the gelatin core facilitated an initial release phase upon hydration, followed by a more gradual hormone diffusion through the surrounding CA layers. The hydrophobicity of CA effectively slowed down water penetration, thereby reducing the rate of hormone diffusion.

Comparative analysis between the pullulan fibers and the multilayered gelatin-CA systems highlighted the capacity to precisely tailor release kinetics through material selection and architectural design. The pullulan system was confirmed to be ideal for fast-dissolving applications, while the multilayered structure offered a promising strategy for sustained delivery.

In conclusion, these chapters highlight the strategic integration of polymer science, drug delivery mechanisms, and nanotechnology in the development of advanced hormone delivery systems. The effective encapsulation, validated through FTIR, TGA, and SEM, along with the improved stability and controlled release profiles, demonstrates the potential of CD-functionalized electrospun nanofibers for both rapid and sustained hormone therapy. This work presents a flexible platform for oral or transmucosal hormone delivery, laying the groundwork for future translational studies and clinical applications.

SİKLODEKSTRİN FONKSİYONLU NANOLİFLERİN HORMON SALIM SİSTEMLERİ OLARAK KULLANIMLARI

ÖZET

Bu tez, hormon salım sistemlerinde kullanılmak üzere siklodekstrin (CD)-fonksiyonelleştirilmiş polimer nanoliflerinin geliştirilmesine odaklanmaktadır. Özellikle, hidrofilik ve hidrofobik polimerlerin rasyonel seçimi, hormonların farklı konsantrasyonlarda entegrasyonu ve CD'lerin dahil edilmesinin ilaç yükleme kapasitesi, stabilite ve salım kinetikleri üzerindeki etkileri araştırılmıştır. Çalışma, hormon yüklü nanoliflerin salım davranışını inceleyerek, hızlı ve sürdürülebilir salım profillerinin elde edilmesini amaçlamaktadır. Pullulan ve jelatin gibi hidrofilik polimerler, hızlı çözünme özellikleri sayesinde hızlı ilaç salınımı sağlarken, hidrofobik selüloz asetat (CA) polimeri, uzun süreli ilaç salımını teşvik etmek için kullanılmıştır. Her formülasyonda, CD'lerin entegrasyonu, hormonların çözünürlük ve stabilitesini artırmak ve aynı zamanda nanolif yapıların içindeki salım profillerini modüle etmek için kullanılmıştır.

Progesteron (P4), estradiol (E2) ve estriol (E3) gibi hormonların oral yolla uygulanması, bu hormonların çeşitli fizyolojik süreçlerde kritik düzenleyici işlevler üstlenmeleri nedeniyle klinik açıdan büyük önem taşımaktadır. Bu steroidal hormonlar, vücutta üretilebilmelerine rağmen, genellikle klinik ortamlarda, vücutta doğal hormon üretimindeki dalgalanmalara, eksikliklere veya işlev bozukluklarına bağlı olarak dış kaynaklardan takviye edilmektedirler.

P4, adet döngüsünü düzenlemede, gebeliği sürdürmede ve embriyo gelişimini desteklemede kritik bir hormondur. Başlangıçta korpus luteum tarafından ve gebelik sırasında daha sonra plasenta tarafından salgılanır. P4, endometriyumu embriyo implantasyonu için hazırlar ve erken gebeliği sürdürür. Ancak, progesteron düzeyleri luteal faz hataları, anovülasyon veya peri- ve postmenopozal kadınlarda hormon replasman tedavisi (HRT) sırasında yetersiz olabilir. P4 takviyesi, yardımcı üreme teknolojileri (ART), luteal faz desteği ve endometrial hiperplazi gibi durumların tedavisinde önemlidir.

E2, en güçlü doğal östrojen olup, üreme sağlığı, kemik yoğunluğunun korunması, kardiyovasküler koruma ve nöroproteksiyon için gereklidir. E2 seviyeleri menopoz sırasında belirgin şekilde azalır, bu da sıcak basmaları, ruh hali değişimleri ve osteoporoz riski gibi semptomlara yol açar. Klinik olarak, E2 menopozdaki kadınlarda HRT, hipogonadizm tedavisi ve ovariyumların cerrahi olarak çıkarılması ya da diğer

tıbbi durumlar sonrasında östrojen eksikliklerinin yönetilmesinde kullanılır.

E3, E2'den daha zayıf bir östrojen olarak kabul edilse de, gebelik sırasında önemli bir rol oynar ve güvenli kullanım profili nedeniyle terapötik potansiyeli giderek daha fazla tanınmaktadır. E3, genellikle güçlü östrojenlere tolerans gösteremeyen kadınlarda HRT'de kullanılır. Dokuya seçici etkinlik gösterir ve endometrial veya meme dokusunu uyarma riski daha düşüktür, bu da onu uzun süreli kullanım için daha güvenli bir alternatif yapmaktadır.

Vücudun bu hormonları sentezleme yeteneği olmasına rağmen, dışarıdan takviye genellikle fizyolojik seviyeleri restore etmek, hormonla ilişkili hastalıkları yönetmek veya yaşa bağlı ya da hastalıkla ilgili endojen üretim düşüşünü telafi etmek için gereklidir. Bu kapsamda, hormonlar oral tablet veya kapsül olarak alındığında, genellikle karaciğerde önemli bir ilk geçiş metabolizmasından geçerler, bu da biyoyararlanımlarını önemli ölçüde azaltır. Dolayısıyla miktar olarak vücutta istenilen miktarın üstünde alınırlar ve dolayısyla alınan fazla ilaçlar vücutta yan etkilere neden olabilmektedirler. Bu doğrultuda tez, CD-fonksiyonelleştirilmiş nanoliflerin kullanımıyla söz konusu zorluklara çözüm üretmeyi hedeflemekte olup, bu yaklaşım hormon salımıyla ilgili engellerin aşılmasına yönelik yenilikçi bir yöntem sunmaktadır. CD'lerin suda çözünmeyen ilaç molekülleriyle inklüzyon kompleksleri oluşturma yeteneği ve elektroeğirme yöntemiyle nanometre kalınlığında ilaç taşıyıcı yapıların üretilebilmesi sayesinde, kontrollü ve ayarlanabilir dozlarda ilaç salımı sağlayan sistemler geliştirilmiştir. Hidrofilik ve hidrofobik polimerlerin tek bir sistemde entegrasyonu, kişiselleştirilmiş ve verimli oral hormon terapisi için potansiyeli artırmaktadır. Tez, elektroeğirme yönteminin temelleri ve hormon taşıma sistemlerinde elektrospun liflerin kullanımı üzerine bir giriş ile başlamaktadır. Ardından, hormon yüklü, CD-fonksiyonelleştirilmiş polimer liflerinin elektroeğirme süreci ve hormon taşıma sistemlerindeki potansiyelleri incelenmektedir. Bunu takiben, kullanılan malzemeler ve gerçekleştirilen deneyler hakkında detaylı bilgi veren deneysel bir bölüm yer almaktadır.

Dördüncü bölümde, seçilen hormonların—P4, E2 ve E3—hidrofilik pullulan bazlı liflerden kapsülasyonu ve salım davranışı araştırılmaktadır. Bu hidrofobik yapıdaki hormonlar, suda düşük çözünürlükleri nedeniyle önce CD'lerle kompleksleştirilmiş ve ardından hidrofilik polimer matrisiyle uyumlarını artırmak için pullulan çözeltileriyle karıştırılmıştır. Elektroeğirme parametrelerinin—polimer konsantrasyonu, akış hızı, voltaj ve iğne-collector mesafesi—optimizasyonu, düzgün, topaksız liflerin elde edilmesi için dikkatlice yapılmıştır. Lif morfolojisi, optik mikroskop ve taramalı elektron mikroskobu (SEM) kullanılarak incelenmiş ve sürekli, düzgün liflerin başarıyla oluşturulduğu ve gözle görülür agregalar veya kristalin hormon kalıntılarının olmadığı doğrulanmıştır. Hormon–CD komplekslerinin lif oluşumunu olumsuz yönde etkilemediği ve polimer matrisiyle iyi uyum gösterdiği gözlemlenmiştir. FTIR analizi, P4, E2 ve E3'ün liflerdeki başarılı kapsülasyonunu, karakteristik hormon piklerini tespit ederek doğrulamıştır.

TGA sonuçları, kapsüle edilmiş hormonların termal stabilitesinin arttığını, ham ilaçlar ve CD kompleksleriyle karşılaştırıldığında daha yüksek bozulma sıcaklıkları gösterdiğini kanıtlamıştır. İn vitro salım çalışmaları, pullulan bazlı sistemlerin ilaç salım kinetiklerini değerlendirmek amacıyla sıvı ortamda gerçekleştirilmiştir. Pullulanın hidrofilik doğası, liflerin simüle tükürük ile temas ettiğinde hızlı bir şekilde dağılmasını sağlamış ve kapsüle edilmiş hormonların anında salımını tetiklemiştir. Bu hızlı salım profili, mukozal membranlar üzerinden hızlı emilim istenen sublingual veya bukkal uygulamalar için özellikle değerlidir. Veriler, hormon salımının dakikalar içinde sağlandığını ve bu sistemlerin hızlı etki başlangıcı gerektiren uygulamalar için ideal olduğunu doğrulamıştır.

Sonraki bölümde, kontrollü hormon salımı sağlamak amacıyla sandviç yapıdaki çok katmanlı lifler üretilmiştir. Bu sistem, dış katmanlar olarak hidrofobik CA ve iç çekirdek katman olarak biyouyumlu, hidrofilik jelatin kullanılmıştır. İç jelatin katmanı, hormon–CD komplekslerini içerirken, CA katmanları, salım hızını modüle etmek için difüzyon engelleri olarak işlev görmüştür. Bu çok katmanlı yapının üretimi, sıralı bir elektrospinning işlemi ile gerçekleştirilmiştir. Her katman, homojenlik ve tekrarlanabilirlik sağlamak için kontrollü kalınlık dikkate alınarak yapılmıştır. Optik mikroskopi, her katmanın lif yapısını incelemek için kullanılmış ve FTIR analizi, hormonların farklı konsantrasyonlarda kapsüllenmesini doğrulamıştır. Salım çalışmaları, jelatin katmanın hidrasyon sonrası ilk salım fazını kolaylaştırdığını ve ardından çevredeki CA katmanlarından daha yavaş bir hormon difüzyonu sağladığını göstermiştir. CA'nın hidrofobikliği, suyun penetrasyonunu etkili bir şekilde yavaşlatmış ve böylece hormon difüzyon hızını azaltmıştır.

Pullulan lifleri ve çok katmanlı jelatin-CA sistemleri arasındaki karşılaştırmalı analiz, materyal seçimi ve mimari tasarım yoluyla salım kinetiklerini hassas bir şekilde özelleştirme kapasitesini ortaya koymuştur. Pullulan sistemi, hızlı çözünen uygulamalar için ideal olarak onaylanmış, çok katmanlı yapı ise sürdürülebilir salım için umut verici bir strateji sunmuştur.

Sonuç olarak, bu bölümler, polimer bilimi, ilaç taşıma mekanizmaları ve nanoteknolojinin stratejik entegrasyonunu, ileri düzey hormon taşıma sistemlerinin geliştirilmesinde vurgulamaktadır. FTIR, TGA ve SEM ile doğrulanan etkili kapsülasyon ve iyileştirilmiş stabilite ve kontrollü salım profilleri, CD-fonksiyonelleştirilmiş nanoliflerin hem hızlı hem de sürdürülebilir hormon terapisi için potansiyelini göstermektedir. Bu çalışma, oral veya transmukozal hormon taşıma için esnek bir platform sunarak, gelecekteki translasyonel çalışmalar ve klinik uygulamalar için temel oluşturmaktadır.

1. INTRODUCTION

Hormone therapy plays a pivotal role in modern medicine, offering effective treatment for numerous conditions such as endocrine dysfunctions, reproductive system irregularities, menopausal symptoms, and other hormone-related health issues. Hormones such as progesterone (P4), estradiol (E2), and estriol (E3) play vital roles in maintaining physiological homeostasis, regulating reproductive cycles, and supporting various metabolic and developmental processes. As such, their therapeutic administration is often indispensable for restoring hormonal balance and improving patient outcomes. However, the clinical effectiveness of hormone therapy is critically influenced by the delivery method employed, which directly affects the pharmacokinetics, therapeutic efficacy, patient compliance, and overall treatment success.

Traditional routes of hormone administration—such as oral tablets, transdermal patches, and intramuscular injections—have demonstrated several limitations. These include poor aqueous solubility of many steroid hormones, first-pass hepatic metabolism, variable absorption rates, and inconsistent plasma concentrations. Additionally, the need for frequent dosing or invasive administration methods can adversely impact patient adherence, especially in long-term therapies. These challenges have accelerated the exploration and development of innovative drug delivery systems that not only improve solubility and stability but also enable controlled and sustained release of hormones, thereby optimizing therapeutic efficiency while minimizing side effects.

In last decades, electrospun nanofibers have garnered significant attention as a next-generation platform for drug delivery due to their unique physicochemical properties. These nanofibers offer an exceptionally high surface-area-to-volume ratio, interconnected porous structure, and tunable mechanical and morphological characteristics, which collectively enable efficient drug encapsulation and customizable release kinetics. The versatility of the electrospinning technique allows for the incorporation of a wide range of bioactive agents, including hydrophobic and

hydrophilic drugs, as well as functional excipients such as cyclodextrins (CDs), thereby providing a multifunctional matrix tailored for advanced therapeutic applications.

CDs are cyclic oligosaccharides composed of glucose subunits, distinguished by a hydrophilic outer surface and a hydrophobic internal cavity. This amphiphilic structure allows them to encapsulate hydrophobic drug molecules within their cavity, forming non-covalent host-guest inclusion complexes (ICs). These complexes significantly enhance the solubility, chemical stability, and bioavailability of hydrophobic drugs, including steroidal hormones, while simultaneously offering protection against hydrolysis, photodegradation, and oxidative processes. Incorporating CDs into nanofiber matrices further augments drug delivery potential by improving drug distribution within the fibers, increasing encapsulation efficiency, and enabling modulation of release behavior through specific CD–drug interactions. Given their excellent safety profile, biocompatibility, and regulatory approval for pharmaceutical use, CDs are particularly advantageous for mucosal drug delivery via sublingual, buccal, and vaginal routes, where rapid absorption and localized delivery are often desired.

The choice of polymer in fabricating CD-functionalized nanofibers plays a pivotal role in determining the mechanical integrity, degradation behavior, and drug release profile of the final formulation. Pullulan, a non-toxic, water-soluble polysaccharide produced by the fungus *Aureobasidium pullulans*, has gained widespread interest in pharmaceutical formulations due to its biocompatibility and rapid solubility in aqueous environments. These attributes make pullulan particularly attractive for oromucosal delivery systems requiring fast disintegration and immediate drug release. However, to achieve more sustained or prolonged hormone release, multilayered nanofiber systems have been developed using complementary polymers with different solubility and permeability characteristics. For instance, combining hydrophobic polymers such as cellulose acetate (CA) with hydrophilic polymers like gelatin (Gel) can result in a sandwich-like fiber structure, where the outer CA layers act as diffusion barriers and the inner Gel layer serves as the primary drug reservoir. This architectural strategy enables fine-tuning of the release profile by regulating drug diffusion and polymer degradation, offering better control compared to single nanofiber systems.

This study aims to fabricate and systematically characterize CD-functionalized nanofibers for the delivery of P4, E2, and E3 hormones, which are central to hormonal regulation, fertility, and gynecological health. These hormones, although clinically valuable, are characterized by poor water solubility and limited stability, which hinder their effectiveness in conventional delivery formats. By usng the unique properties of CDs and electrospun nanofibers, this research seeks to overcome these limitations and create novel delivery vehicles that enhance hormone solubilization, stability, and bioavailability. Furthermore, the effect of different CD types, molar ratios, and polymer compositions on fiber morphology, drug encapsulation efficiency, and release kinetics are evaluated.

Ultimately, this work aspires to contribute to the advancement of personalized hormone therapy by providing flexible and efficient delivery platforms tailored to individual therapeutic needs. The insights derived from this investigation may also pave the way for broader applications of nanofibrous systems in the delivery of other poorly soluble drugs, fostering innovation in non-invasive, controlled-release drug delivery strategies across multiple therapeutic domains.

2. THEORETICAL PART

2.1 Electrospinning

Electrospinning is one of the most versatile techniques used in generating polymeric nanofibers from a diverse range of polymeric materials, both synthetic and natural, while preserving their chemical properties (Ahmed vd., 2015). It consists of applying a high electric field to a polymer solution jet in order to obtain nano- and microfibers with diameters ranging from a few nanometers to several micrometers (Bhardwaj & Kundu, 2010).

These electrospun nanofibers possess a high surface area-to-volume ratio, high porosity, tunable wettability, and the capability to functionalize with different molecules, making them quite an attractive choice for nanocatalysis, drug delivery, food packaging, tissue engineering, filtration, and supercapacitors (Bottino, 2016; Hu vd., 2014). The key parameters that affect the final properties of the resulting nanofibers are the properties of the polymer solution (*e.g.*, conductivity, surface tension, and viscosity), the voltage applied, the flow rate, and the distance between the spinneret and the collector (Al-Abduljabbar & Farooq, 2023). At the same time, formulation parameters like solution concentration had the most significant impact on electrospinnability, leading to a shift from electrosprayed beads to electrospun fibers (Deitzel vd., 2001). The solvent chosen for preparing the polymer solution should possess an appropriate vapor pressure to ensure the structural integrity of the electrospun fibers: A low boiling-point solvent can evaporate quickly, hindering polymer elongation and resulting in clogged needles or an unstable Taylor cone (Sarkar vd., 2010) (Balgis vd., 2018).

In 1934, Formhals pioneered the electrospinning technique by inventing a device that used electrostatic force to produce polymer fibers (Zhao vd., 2020). This marked the beginning of electrospinning technology. However, the development of this technique stagnated between 1964 and 1969 due to the lack of tools to accurately measure the

sub-micrometer fibers produced (Xue vd., 2019). During this time, Geoffrey Taylor's groundbreaking work provided a mathematical model to describe the shape change of polymer solutions under strong electric fields. Over time, electrospinning has evolved, and researchers have developed various modifications, such as needleless electrospinning, coaxial or triaxial electrospinning, and multi-jet electrospinning, to enhance its capabilities (Altan vd., 2018).

The key components for the electrospinning technique include a high voltage source, a metal needle, and a conductive collector (Zhao vd., 2020). The polymer solution is expelled from the capillary tube by the electric field, often resulting in the formation of a Taylor cone at the capillary tip. Increasing the electric field strength causes positive charges to build up on the surface of the Taylor cone, overcoming the surface tension and enabling the polymer jet to accelerate towards the collector (Figure 2.1).

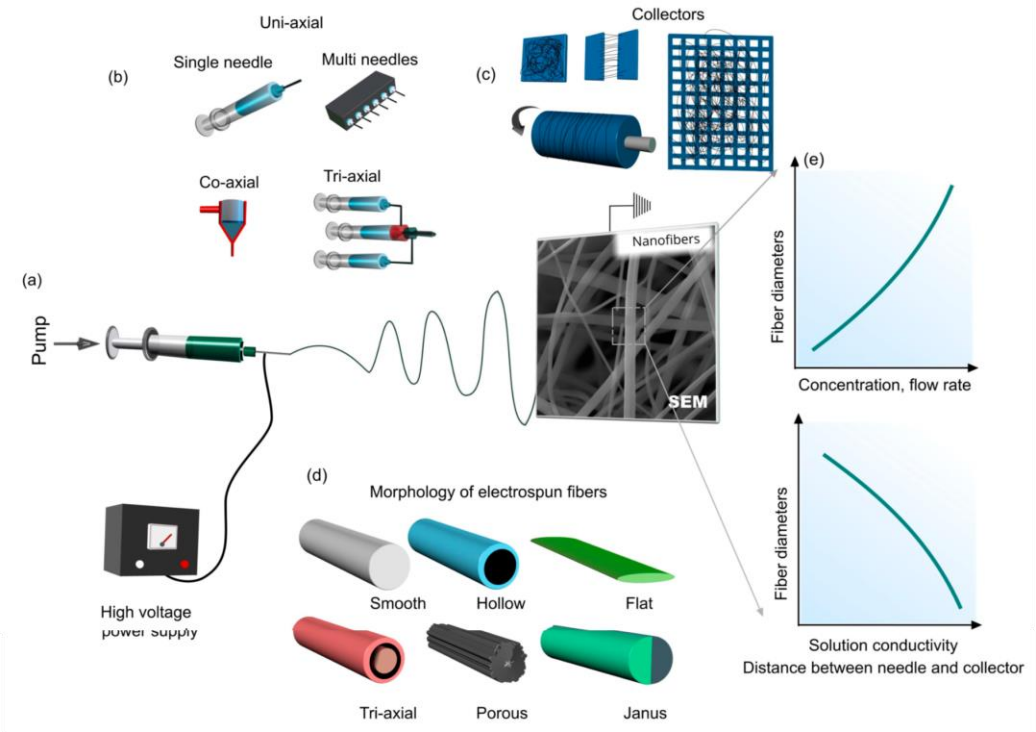

Figure 2.1: The electrospinning setup and key parameters are illustrated, including (a) a schematic representation of an electrospinning system alongside a scanning electron micrograph of electrospun fibers, (b) typical spinneret configurations used in electrospinning, (c) various collector designs, (d) examples of electrospun fiber morphologies, and (e) diagrams depicting the effects of solution properties and electrospinning process parameters on the fiber diameter of the resulting fibers. The figure was reproduced from (Topuz & Uyar, 2019) with permission of MDPI.

Contemporary research in electrospinning focuses on innovative polymer blends, functional additives, and the fine-tuning of process parameters to improve the performance and quality of electrospun nanofibers for a wide range of emerging applications (Li vd., 2021). Advances in specialized electrospinning equipment and the application of sophisticated characterization techniques have empowered researchers to gain deeper insights into the intricate relationship between processing conditions and the resulting nanofibers' morphology, mechanical properties, and functionality (Rutledge & Fridrikh, 2007)

2.2 Electrospun Fibers for Hormone Delivery

Electrospun fibers have emerged as a promising platform for oral hormone delivery, offering high surface area, tunable porosity, and the ability to encapsulate a variety of therapeutic agents (Özen & Wang, 2023). These nanofibers enable controlled and sustained drug release, improving patient compliance and minimizing side effects. By incorporating CDs, researchers have developed fast-dissolving systems to enhance the bioavailability of poorly water-soluble drugs (Topuz & Uyar, 2019). Several hormones, such as progesterone (P4), estradiol (E2), and estriol (E3), have been studied for delivery through electrospun nanofibers, with various polymers and release mechanisms designed to enhance stability and efficacy. For instance, a study on P4-loaded polycaprolactone nanofibers showed a dual-phase release (Almousained vd., 2024). Likewise, another investigation into estradiol-loaded poly(ε-caprolactone) and silk fibroin fibers highlighted a biphasic release pattern, essential for treating osteoporosis (Steffi vd., 2018). Additionally, CA nanofibers were developed for P4 delivery, demonstrating a burst release followed by sustained release, with the release mechanism dependent on drug concentration (do Nascimento Soares vd., 2020).

When comparing oral hormone delivery to transdermal methods, significant differences in hormonal bioavailability and metabolism exist. Oral estrogens undergo first-pass metabolism in the liver, potentially causing variations in hormone levels and increasing the risk of venous thromboembolism (Goodman, 2012). In contrast, transdermal estrogen administration has little or no effect on venous thromboembolism risk (“Committee Opinion No. 556”, 2013). While oral hormone delivery is

convenient, healthcare providers must consider individual patient factors, risks, and benefits when selecting the most appropriate administration method.

Sublingual and buccal hormone delivery *via* electrospun nanofibers are gaining attention for their potential in overcoming the limitations of traditional oral drug administration. These routes enable rapid drug absorption directly into the circulation, bypassing the first-pass metabolism in the liver, which is particularly beneficial for drugs with low oral bioavailability. Both sublingual and buccal delivery can also provide faster onset of action. Additionally, hormone-loaded fibers for vaginal delivery offer an alternative for sustained drug release, providing localized and prolonged therapeutic effects, which can be particularly useful for conditions like hormone replacement therapy.

However, there are challenges associated with these delivery methods. For sublingual and buccal routes, the formulation must remain stable and adhere well to the mucosal membranes to ensure sufficient absorption time (Morales vd., 2017). Local irritation or discomfort may also arise, particularly with certain drugs or polymers. Saliva production and the swallowing reflex can also impact drug release. For vaginal delivery, while it can provide sustained release, ensuring the fibers' proper adhesion and retention in the vaginal environment is critical (Blakney vd., 2013). Despite these challenges, electrospun fiber-based delivery systems for sublingual, buccal, and even vaginal routes hold promise for providing fast-acting, efficient, and sustained hormone delivery options.

2.3 Cyclodextrin-based Drug Delivery Systems

CD-based drug delivery systems utilize cyclic oligosaccharides known as CDs, composed of glucopyranose units linked by α-1,4 glycosidic bonds. α-, β-, and γ-CDs are common types, consisting of 6, 7, and 8 glucose units respectively (Topuz & Uyar, 2024). Their unique molecular structure features a hydrophilic exterior and a hydrophobic interior cavity, ideal for encapsulating hydrophobic drug molecules (Figure 2.2).

The ability of CDs to form host-guest ICs enables improved solubility of poorly water-soluble drugs. Furthermore, CDs can protect encapsulated drugs from environmental degradation, such as hydrolysis, oxidation, or photolysis, thereby extending the drug's

shelf life (Loftsson vd., 2005). Natural CDs form strong hydrogen bonds, resulting in moderate or low water solubility. To enhance their solubility, functional groups have been introduced through chemical modifications. As a result, CDs have been functionalized with various groups, including hydroxypropyl (HP), methyl (M), sulfobutylether (SBE), and carboxymethyl (CM) (Topuz & Uyar, 2024), allowing for enhanced targeting, controlled drug release, and improved interaction with biological systems. These versatile features position CD-based materials as a promising platform for advanced drug delivery systems (Vyas et al., 2008).

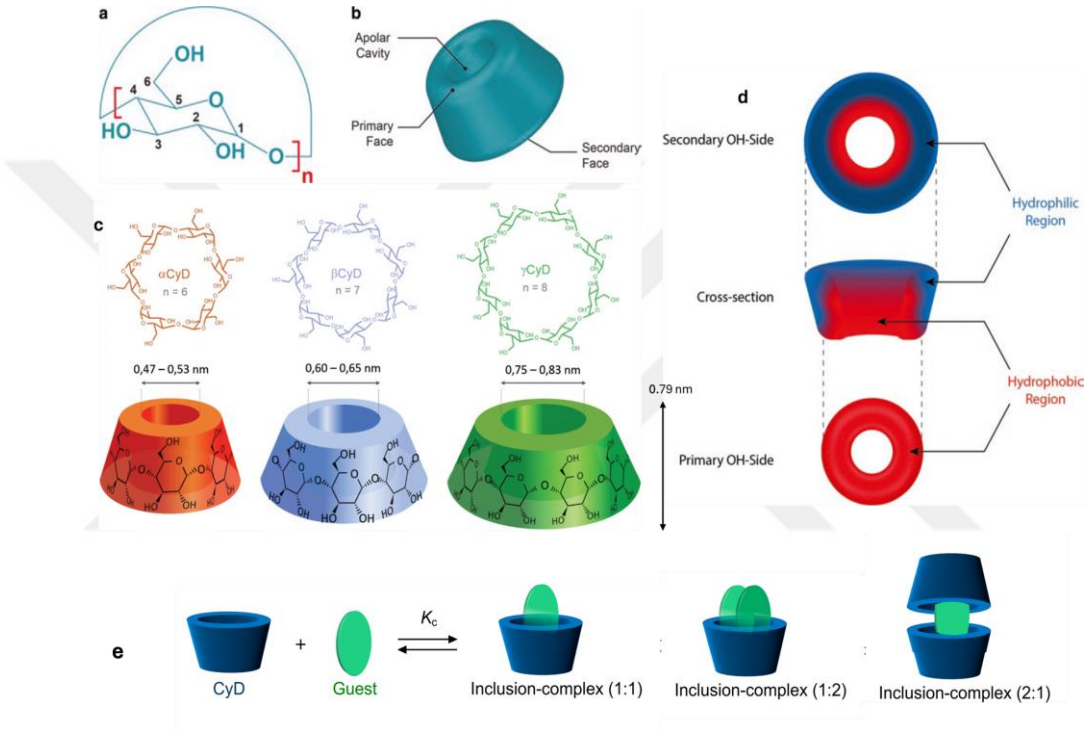

Figure 2.2: Diagrammatic representation of (a) the general chemical structure of cyclodextrins (CDs) and (b) their distinctive toroidal shape, emphasizing the hydrophobic inner cavity and hydrophilic exterior. (c) chemical 3-dimensional structure and dimensions for α-, β-, and γ-CDs (n = 6, 7, and 8, respectively) (d) CD "capsule" showing the hydrophobic and hydrophilic regions. (e) The IC formation between CD and guest molecules at various stoichiometries. Figure was reproduced from (Agnes vd., 2022), (Topuz & Uyar, 2019) and (Morin-Crini vd., 2020) with permission from Wiley, MDPI and Springer.

In the context of electrospun nanofibers, CDs offer significant advantages for hormone delivery. By incorporating CDs into electrospun fibers, the solubility and stability of hydrophobic hormones can be greatly enhanced, allowing for more efficient loading and sustained release. The inclusion of CDs in electrospun fibers helps optimize the release profiles of hormones, ensuring that they remain stable and bioavailable during

the delivery process. Additionally, CDs' ability to form ICs with hormones can improve the controlled release of drugs (Albers & Müller, 1992; Araj & Szeleszczuk, 2023; K. vd., 1982), offering a more targeted and effective hormone delivery system. This combination of electrospun fibers and CD-based technology enhances the potential for developing advanced, efficient, and stable hormone delivery platforms for various therapeutic applications.

2.4 Rapid Hormone Delivery from Electrospun Pullulan Fibers

Polysaccharides like starch, chitosan, alginate, and pullulan are widely used in the development of biomaterials due to their stability, non-toxicity, biocompatibility, and biodegradability (Celebioglu & Uyar, 2021; Ertan vd., 2023). Notably, pullulan stands out for biomaterial design due to its hydrophilic nature and unique properties.

Pullulan is a biopolymer produced through the industrial fermentation of starch syrup by the yeast-like fungus *Aureobasidium pullulans* (Singh vd., 2008), It is a microbial exopolysaccharide comprising maltotriose units linked by α-(1,4) and α-(1,6) glycosidic bonds (Grenha & Rodrigues, 2013). Pullulan is odorless, tasteless, non-toxic, highly water soluble due to the low degree of hydrogen bonding, and stable under temperature and pH changes (Tatiana Román vd., 2019). It can improve the solubility and bioavailability of hydrophobic pharmaceuticals (Mauri et al., 2018). These distinctive characteristics that render it well-suited for oral drug delivery applications (Raghav vd., 2020). Electrospun pullulan nanofibers have shown promise for drug delivery (Asgari vd., 2021; Hsiung vd., 2022; Mehdi vd., 2021), cosmetics (Coltelli vd., 2020; Tatiana Román vd., 2019), food packaging (Celebioglu & Uyar, 2021) and many other fields. While recent research has explored vaginal administration of P4-loaded pullulan nanofibers (Lavanya vd., 2024), their potential application as oral delivery systems for steroid hormones remains a novel and largely unexplored area.

P4, a steroid hormone predominantly produced by the corpus luteum and the placenta (Taraborrelli, 2015), is a crucial regulator of the female reproductive system, particularly the menstrual cycle, embryogenesis and pregnancy (Lavanya vd., 2024). As the only FDA-approved drug for preventing preterm birth, its therapeutic importance is well-established. Synthetic versions of P4, known as progestins, are also

widely used in hormone replacement therapy for conditions such as menopause, primary ovarian insufficiency, endometriosis, and luteal deficiency (Franklin, 2020). It can also be administered alongside estrogen in contraceptive formulations to help lower the risk of developing uterine or cervical cancer (Matencio vd., 2024).

E2, the most potent and physiologically active form of estrogen, is predominantly synthesized by the ovaries and exerts a multifaceted influence on the female organism. It serves as a key regulator in the development and maturation of the female reproductive system, stimulating the growth and proliferation of uterine and vaginal tissues (Wetendorf & DeMayo, 2012). Additionally, E3 has been observed to significantly impact the skeletal system, reducing adipose tissue and modulating body weight, as well as the nervous system, where it has been implicated in the treatment of neurodegenerative conditions such as Parkinson's and Alzheimer's disease (Aubead, 2021; Young, 2013).

E3, a less potent estrogen than E2, is primarily secreted by the placenta during pregnancy. Its concentrations increase substantially throughout gestation, peaking immediately before birth (Klausner & Ryan, 1964). This estrogenic hormone plays a vital role in preparing the uterus for the birthing process, facilitating the softening and dilation of the cervix, as well as stimulating uterine contractions (Levitz & Young, 1978).

Incorporating CDs or their derivatives as ICs with hormones, can further enhance the solubility and stabilization of the hydrophobic hormones as previous reports demonstrated (Aytac et al., 2015). The formation of the host-guest complex between the CD and the hormones can improve the bioavailability of the hormones and facilitate their disintegration. In this context, this thesis investigates the utilization of pullulan-based electrospun nanofibers as a delivery platform for the rapid release of steroid hormones (*i.e.*, P4, E2, and E3) (Table 2.1).

In chapter 4, the encapsulation efficiency of the steroid hormones within the pullulan nanofibers was determined, and their *in vitro* release profiles were investigated. To further characterize the properties of this delivery system, TGA was utilized to evaluate the thermal properties of the nanofibers. Additionally, SEM and FTIR were employed to assess the morphology and structural characteristics of the nanofibers. The release amount of the hormones was quantified using UV-Vis spectrophotometry.

Table 2.1: Chemical properties and structures of P4, E2 and E3 hormones.

Hormone	Abb	Source	Molecular Formula	Molar Mass (g/mol)	IUPAC name	Chemical Structure
Progesterone	P4	Corpus luteum, placenta	$C_{21}H_{30}O_2$	314.469	Pregn-4-ene-3,20-dione	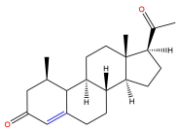
Estradiol	E2	Ovaries	$C_{18}H_{24}O_2$	272.38	Estra-1,3,5(10)-triene-3,17ß-diol	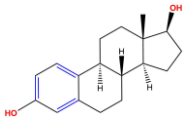
Estriol	E3	Placenta (during pregnancy)	$C_{18}H_{24}O_3$	288.387	Estra-1,3,5(10)-triene-3,16a,17ß-triol	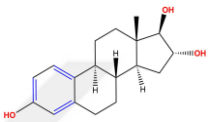

2.5 Sustained Hormone Delivery from Sandwich Electrospun Fibers

Gel is a protein-based polymer obtained through the partial hydrolysis of collagen, which is found in the skin and connective tissues of animals. Its biocompatibility, biodegradability, and cell-binding capabilities have been extensively researched (Liao vd., 2006). Gel is known for its gelling and thickening properties, making it a popular ingredient in food and pharmaceutical industries (Tofanica vd., 2022). Gel-based nanofibers have demonstrated the ability to encapsulate and release a range of therapeutic agents, such as drugs, proteins, and growth factors, in a controlled manner (Morais vd., 2023). On the other hand, CA is a synthetic polymer derived from cellulose, a natural polysaccharide that is the primary component of plant cell walls. It is primarily used in the production of textiles, plastics, and photographic films (Tofanica vd., 2022). Due to its mechanical strength, chemical stability, and drug permeability properties, CA-based nanofibers have been investigated as a drug delivery system (Khoshnevisan vd., 2018; Wsoo vd., 2020).

The multi-layer structure could be engineered to provide controlled and sustained hormone release, with the hydrophobic outer layers acting as a barrier to slow down the hormone release, and the hydrophilic middle layer allowing for the gradual diffusion of the encapsulated hormones. The incorporation of CDs in the formulation

represents a strategic decision, as they have the potential to enhance the solubility, stability, and bioavailability of the encapsulated hormones. Furthermore, the multi-layered nanofiber design, with its tailored hydrophobic-hydrophilic properties, is anticipated to provide improved control over the release kinetics of the hormones compared to single-layer systems (Zamani vd., 2013).

Chapter 4 also reports on a multi-layered nanofiber drug delivery system designed for the sustained release of the hormones P4, E2, and E3. The system consists of three distinct layers: the outer layers are made of the hydrophobic polymer CA, while the middle layer is composed of the hydrophilic polymer Gel. The Gel middle layer is loaded with HP-β-CD and HP-γ-CD ICs, with the three hormones at two different molar ratios (0.5:1 and 1:1 (hormone: CD)). The morphology of the resulting fibers was examined through optical microscopy, while the presence of drugs within the fiber was studied through FTIR. The thermal stability of the fibers was explored through TGA. The disintegration of the fibers in simulated saliva was followed over time, while the release of the encapsulated hormones from these sandwich fiber films was monitored through UV-vis spectroscopy.

3. EXPERIMENTAL PART

3.1 Materials

HP-β-CD (Cavasol W7 HP Pharma, Ashland Industries, Switzerland), HP-γ-CD (Cavasol W8 HP Pharma, Ashland Industries, Switzerland), pullulan (Tokio Chemical Industry Co Ltd., Japan), cellulose acetate, progesterone (P4, Sigma Aldrich), estradiol (E2, Sigma Aldrich) and estriol (E3, Sigma Aldrich) were purchased and used as received. Electrospinning solutions were formulated using ultrapure water obtained from a Millipore Milli-Q purification system.

Table 3.1: Compositions and properties of electrospinning solutions containing P4/CD ICs and Pul.

Polymer	CD type	Conc. (% w/v) [a]	P4/CD molar ratio	P4 Conc. (% w/w) [b]	Conductivity (µs/cm)
Pul	HP-β-CD	20/20	0.5:1	5.6	235
Pul	HP-β-CD	20/20	1:1	11.2	85
Pul	HP-γ-CD	20/20	0.5:1	5.1	224
Pul	HP-γ-CD	20/20	1:1	10.21	43
Pul	CD-free	20	0.5:1	10.21	253
Pul	CD-free	20	1:1	20.42	239

[a] with respect to solvent (water); [b]with respect to total sample amount.

3.2 Preparation of Electrospinning Solutions for Fast-disintegrating Fibers

P4/HP-β-CD ICs were prepared at 0.5:1 and 1:1 molar ratios (drug: HP-β-CD), yielding solutions with ~5.6% and 11.2% (w/w) drug content, respectively. 200 mg HP-β-CD (20% w/v) and 200 mg Pul (20% w/v) were dissolved in 1 mL distilled water. P4 was added according to the desired molar ratio and stirred overnight at room temperature. The same procedure was followed using HP-γ-CD instead of HP-β-CD, with the identical molar ratios (0.5:1 and 1:1) which resulted with ~5.1% and 10.21% (w/w) drug content. Pul/P4 control samples were prepared without CDs, maintaining

the same drug ratios as the HP-γ-CD/P4 IC's (0.5:1 and 1:1) that correspond to (10.21 % and 20.42 % w/w) (Table 3.1). The same approach was used to prepare CD/E2 and CD/E3 ICs solutions with Pul (Tables 3.2 and 3.3).

Table 3.2: Compositions and properties of electrospinning solutions containing E2/CD ICs and Pul.

Polymer	CD type	Conc. (% w/v) [a]	E2/CD molar ratio	E2 Conc. (% w/w) [b]	Conductivity µs/cm
Pul	HP-β-CD	20/13	0.5:1	3.9	-
Pul	HP-β-CD	20/13	1:1	7.8	-
Pul	HP-γ-CD	20/13	0.5:1	3.54	-
Pul	HP-γ-CD	20/13	1:1	7.07	-
Pul	CD-free	20	0.5:1	5.9	146
Pul	CD-free	20	1:1	11.79	163

[a] with respect to solvent (water); [b] with respect to total sample amount.

Table 3.3 Compositions and properties of electrospinning solutions containing E3/CD and Pul.

Polymer	CD type	Conc. (% w/v) [a]	E3/CD molar ratio	E3 Conc. (% w/w) [b]	Conductivity µs/cm
Pul	HP-β-CD	20/13	0.5:1	3.9	-
Pul	HP-β-CD	20/13	1:1	7.8	-
Pul	HP-γ-CD	20/13	0.5:1	3.54	-
Pul	HP-γ-CD	20/13	1:1	7.07	-
Pul	CD-free	20	0.5:1	5.9	80
Pul	CD-free	20	1:1	11.79	83

[a] with respect to solvent (water); [b] with respect to total sample amount.

3.3 Electrospinning for Pullulan Fibers

Each solution was loaded into a 1 mL syringe fitted with a 20-gauge blunt-tip needle and positioned horizontally on the electrospinning setup. The environmental conditions were maintained at 22 ± 2 °C and 40 ± 5% relative humidity. A high voltage of 17.5 kV was applied to the stainless-steel needle, while the solution was

pumped at a constant rate of 0.5 mL/h. The electrospun mats were collected on a metal plate positioned 10 cm from the needle tip. The remaining solution from the electrospinning is used to measure the solutions conductivity using a Conductivity-meter.

3.4 Electrospinning for Sandwich Fibers

To create multilayer sandwich-like structures, we used a multi-step process involving CA for the outer layers and hormone/CD ICs loaded Gel for the inner layers. For the outer layers, 200 mg of CA was dissolved in a solution of acetic acid and water (8:2 ratio) for both P4 and E2 sandwiches while 250 mg of CA was used for E3 sandwiches. For the inner layers, nine different solutions were prepared (Table 3.4). First, 300 mg of Gel was dissolved in a 3:7 acetic acid/water mixture. Then, for each type of CD, three separate solutions were created, one for each hormone (P4, E2, and E3). For the CD-containing solutions, 200 mg of either HP-β-CD or HP-γ-CD was added to the Gel mixture. Then, the hormones were added in a 1:1 molar ratio with the CD, which resulted in 44.9 mg P4, 38.9 mg E2, and 41.2 mg E3 for HP-β-CD solutions and 40.8 mg P4, 35.4 mg E2, and 37.45 mg E3 for HP-γ-CD solutions. For the control solutions, the same hormone amounts used in the HP-γ-CD solutions were added to the Gel mixture without CD. Finally, all solutions were stirred at room temperature for 24 hours in order to produce the tri-layered sandwich structure with electrospinning, a specific process was followed. For the base layer, 500 μL of CA solution was electrospun onto the aluminum foil-covered collection plate, forming the first hydrophobic outer layer. Next, 1 mL of the hormone/CD-loaded Gel solution was electrospun directly onto the first layer, creating the hydrophilic inner layer containing. Finally, another 500 μL of CA solution was electrospun, forming the second hydrophobic outer layer and sandwiching the active layer. This tri-layered electrospinning process, using CA for the outer layers and hormone/CD-loaded Gel for the inner layer, was repeated for each of the nine solutions: P4, E2, and E3, each with HP-β-CD, HP-γ-CD, and without any CD. The electrospinning process was conducted under controlled environmental conditions: 22 ± 2°C and 40 ± 5% relative humidity. A high voltage of 17.5 kV was applied to the needle, and the solution was pumped at a constant rate of 0.5 mL/h and TCD of 10 cm.

Table 3.4: Composition and properties of sandwich electrospun films produced using CA and Gel and three different hormones.

Polymer	Layer #	V (ml)	CD type	Conc (% w/v)	Solvent	Volume ratio (v/v)	Hormone	Hormone/CD molar ratio	Conductivity (µs/cm)
CA	1,3	0.5,0.5	-	20	AcOH/H_2O	8:2	-	-	241
Gel	2	1	HP-β-CD	30/20	AcOH/H_2O	3:7	P4	1:1	1287
Gel	2	1	HP-γ-CD	30/20	AcOH/H_2O	3:7	P4	1:1	1232
Gel	2	1	CD-free	30	AcOH/H_2O	3:7	P4	1:1	1976
CA	1,3	0.5,0.5	-	20	AcOH/H_2O	8:2	-	-	241
Gel	2	1	HP-β-CD	30/20	AcOH/H_2O	3:7	E2	1:1	1459
Gel	2	1	HP-γ-CD	30/20	AcOH/H_2O	3:7	E2	1:1	1419
Gel	2	1	CD-free	30	AcOH/H_2O	3:7	E2	1:1	2420
CA	1,3	0.5,0.5	-	25	AcOH/H_2O	8:2	-	-	245
Gel	2	1	HP-β-CD	30/25	AcOH/H_2O	3:7	E3	1:1	1468
Gel	2	1	HP-γ-CD	30/25	AcOH/H_2O	3:7	E3	1:1	1422
Gel	2	1	CD-free	30	AcOH/H_2O	3:7	E3	1:1	2560

3.5 Characterization

The conductivity of the solutions was measured using a Horiba LAQUA portable conductivity meter. Measurements were performed in triplicate, and the average values were reported. The fibers' morphology was examined using an optical microscope and scanning electron microscopy (Thermo Scientific Apreo S). Before SEM analysis, the fiber samples were coated with a thin layer of Pd/Pt. FTIR spectra of the samples were recorded using an FTIR spectrometer (Thermo Scientific Nicolet 380) equipped with an ATR module. The spectra were collected in the range of 4000 to 400 cm^{-1} with a resolution of 4 cm^{-1} and presented in absorption mode. Thermal properties of the fibers and their components were evaluated using a simultaneous thermogravimetric analyzer (TA Instruments SDT Q600). The samples were thermally ramped from ambient temperature to 600 °C at a heating rate of 10 °C per minute.

3.6 Hormone Release Tests

The release tests of the nanofibers of Pul/hormone-HPβCD-IC, Pul/hormone-HPγCD-IC and Pul/hormone for P4, E2 and E3, as well sandwich fibers were measured using a double-beam UV/vis spectroscopy (P9, VWR). For this, ~5 mg of each sample was dissolved in 3 mL of distilled water. The UV/vis spectra were recorded over a defined time period. (λ_{max} =247.5 nm, 280 nm and 280 nm for P4, E2 and E3 respectively). This allowed for the precise measurement of hormone release kinetics from the fibers. Calibration curves of hormone-CD ICs in water were taken with linearity and acceptability of $R^2 \geq 0.99$ and the experiments were repeated two times and an average value was obtained.

3.7 Fiber Disintegration Tests

The disintegration profiles of Pul/hormone-HP-β-CD-IC, Pul/hormone-HP-γ-CD-IC and Pul/hormone for P4, E2 and E3 nanofibers, as well sandwich fibers were followed in simulated saliva (2.38 g Na_2HPO_4, 0.190 g KH_2PO_4, 8 g NaCl in 1L distilled water and adjusting of pH to 6.8 with phosphoric acid) and on saliva-wetted tissues to simulate disintegration in the oral cavity. For this, petri dishes (10 cm) and nanofiber

samples of dimensions ~ 1 x 1.5 cm were used. The dissolution of mats was captured on video and converted into photographs.

4. RESULTS AND DISCUSSION

4.1 Pullulan-based Nanofibers for Rapid Delivery of Hormones

4.1.1. Progesterone delivery

The solutions, regardless of their stoichiometric composition, exhibited opaqueness (Figure 4. 1). Solutions devoid of CDs were also opaque. These solutions were electrospun into fibrous films, which exhibited favorable physical properties, including both flexibility and mechanical strength (Figure 4.1). The mats were foldable without any noticeable deformation. Microscopic analysis revealed slightly beaded fibers, with thinner fibers observed in the absence of CDs (HP-β-CD and HP-γ-CD).

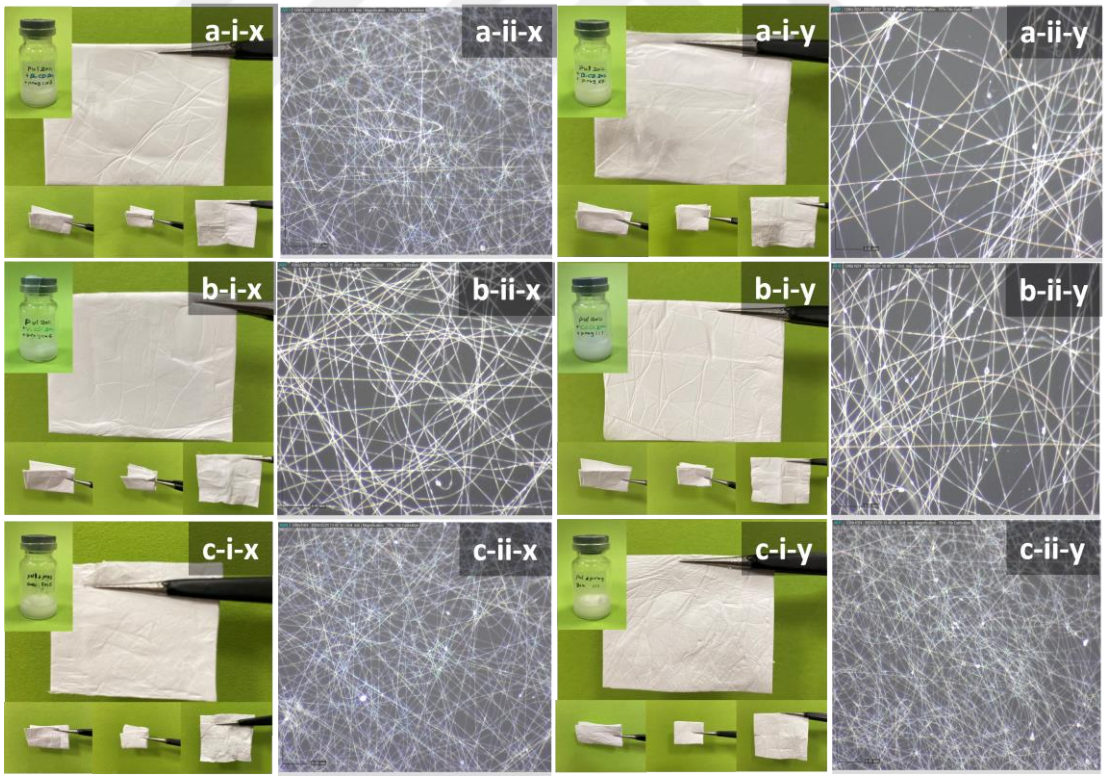

Figure 4.1: (i) Photos of electrospinning solutions, electrospun mats and (ii) microscopic images of (a) Pul/P4/HP-β-CD IC, (b) Pul/P4/HP-γ-CD IC, (c) Pul/P4 at different drug: CD (x) 0.5:1 and (y) 1:1 stoichiometries.

SEM analysis revealed slightly beaded fibers, as shown in the microscopic images in Figure 4.2. Notably, fibers without CD exhibited smaller diameters compared to those containing either type of CD. A 1:1 P4:CD molar ratio resulted in fibers that were thicker and exhibited a more pronounced beaded appearance compared to fibers produced at a 0.5:1 P4:CD molar ratio. In the absence of CDs, P4-loaded Pul fibers had average diameters of 282±49 nm and 254±42 nm for the 0.5:1 and 1:1 molar ratios, respectively. P4/HP-β-CD-loaded Pul fibers at 0.5:1 and 1:1 molar ratios exhibited diameters of 517±79 nm and 724±83 nm, while P4/HP-γ-CD-loaded Pul fibers had diameters of 531±64 nm and 842±188 nm, respectively.

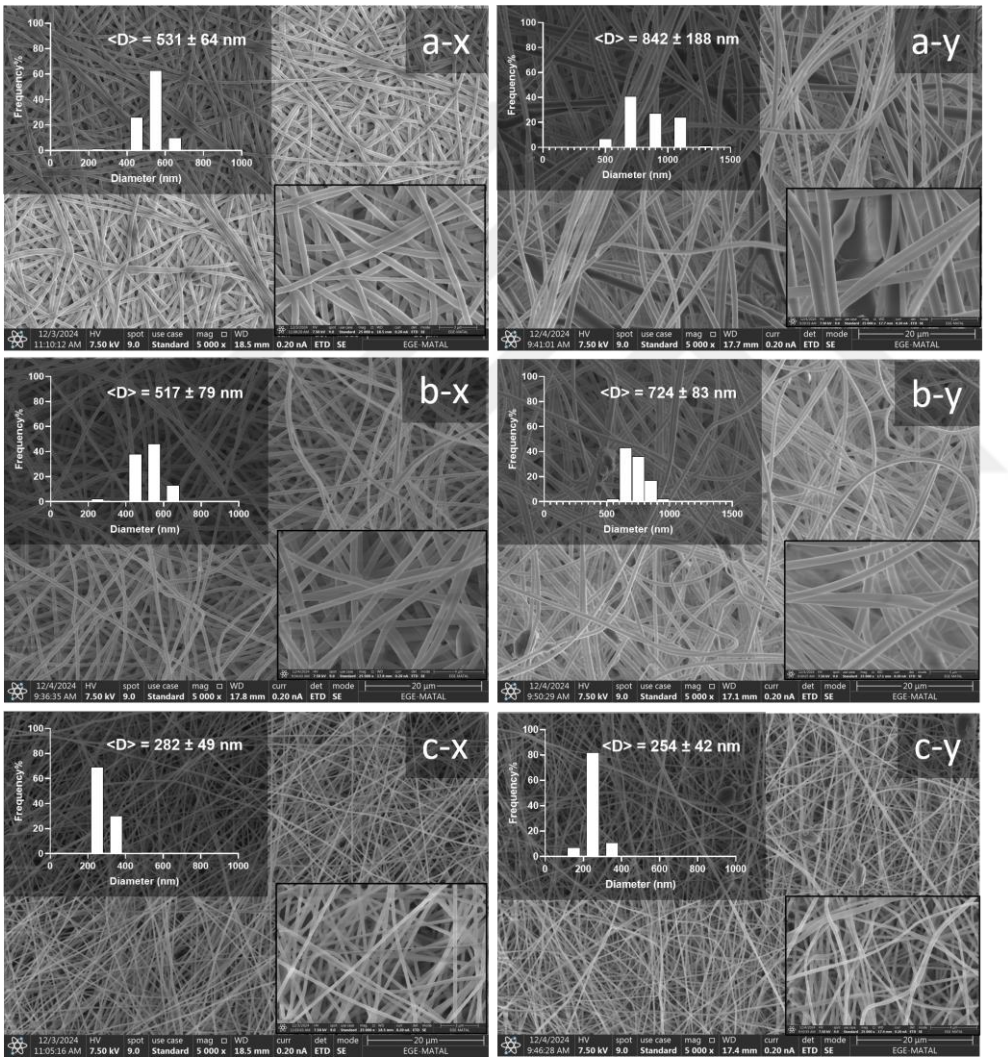

Figure 4.2: Scanning electron micrographs and diameter distribution histograms of (a) Pul/P4/HP-β-CD IC, (b) Pul/P4/HP-γ-CD IC, (c) Pul/P4 at different P4: HP-CD (x) 0.5:1 and (y) 1:1 stoichiometries.

The FTIR spectra compare various samples containing P4, Pul, and CD at two different molar ratios (0.5:1 and 1:1) (Figure 4.3). FTIR spectrum of P4 shows the

characteristics peaks to the ketone stretch around 1690 and 1660 cm^{-1}. The C–H stretching bands between 2950 and 2850 cm^{-1} and CH_2/CH_3 bending vibrations in the range of 1450–1400 cm^{-1} were also detected. On the other hand, both CDs (HP-β-CD and HP-γ-CD) show broad peaks around 3400 cm^{-1} due to O–H stretching and distinctive peaks in the 1000–1200 cm^{-1} region attributed to C–O stretching. The Pul spectrum features a broad peak around 3300 cm^{-1} and shows a relatively smooth profile with characteristic polysaccharide peaks in the fingerprint region (< 1450 cm^{-1}). For the fibers of Pul/P4/CD, the spectra demonstrate features from both CD and P4, with some P4 peaks being reduced, suggesting incorporation of P4 within fibers.

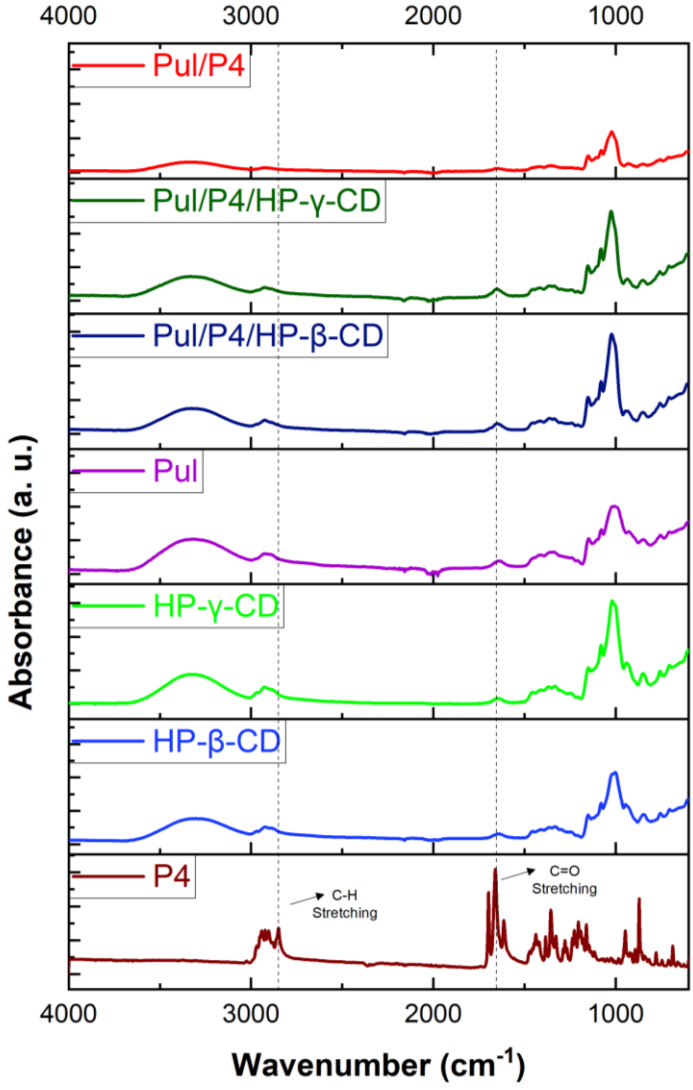

Figure 4.3: FTIR spectra presented from bottom to top: P4, HP-β-CD, HP-γ-CD, Pul, P4/HP-β-CD-loaded Pul NFs, P4/HP-γ-CD-loaded Pul NFs, and P4-loaded Pul NFs at a (0.5:1 - P4:CD molar ratio).

TGA results describe the thermal stability and decomposition behavior of P4, HP-β-CD, HP-γ-CD, Pul, and their nanofiber formulations. P4 exhibited a one-stage decomposition between 150°C and 250°C, reflecting lower thermal stability (Figure 4.4). HP-β-CD and HP-γ-CD decomposed in the temperature range of 300°C to 350°C due to the decomposition of glucopyranose rings. HP-γ-CD exhibited slightly higher thermal stability compared with HP-β-CD. Pul showed two major mass losses: (i) water loss between 100–150°C and (ii) degradation of the backbone between 280 and 350°C. P4/HP-β-CD-loaded Pul nanofibers and P4/HP-γ-CD-loaded Pul nanofibers exhibited enhanced thermal stability compared to pure P4, showing decomposition temperatures matching the Pul and CD degradation at ~300–350°C. P4/CD-free Pul nanofibers degraded at an earlier temperature (~250–300°C) compared to the CD-loaded systems, indicating weaker stabilization in the absence of CDs.

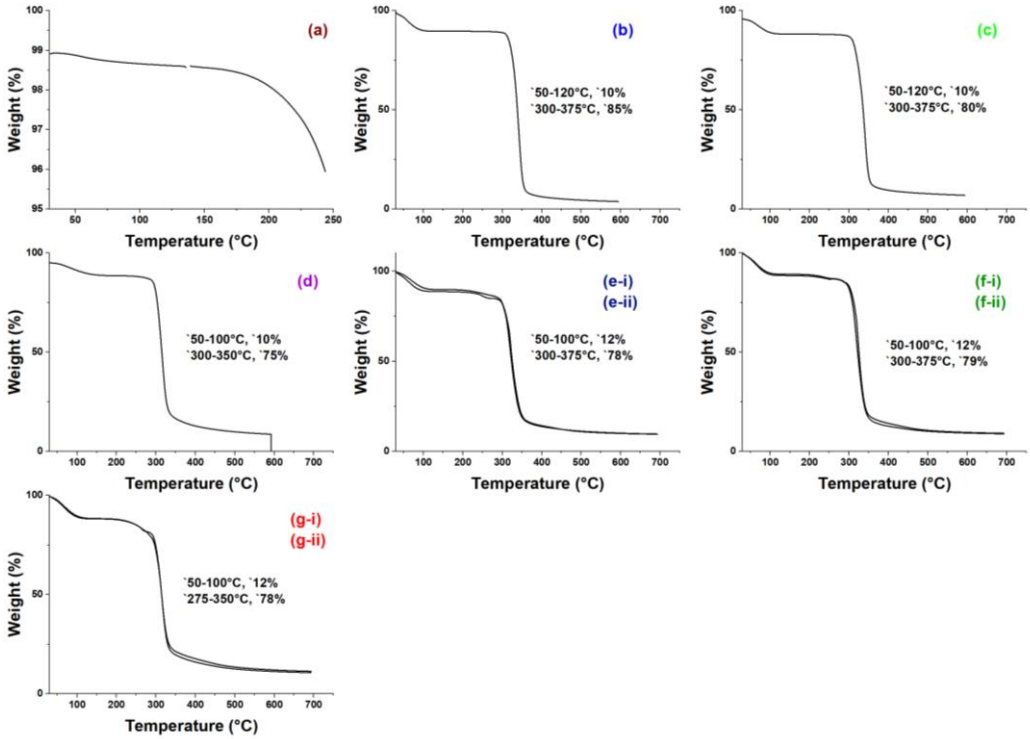

Figure 4.4: The thermogravimetric analysis (TGA) of (a) pure P4, (b) HP-β-CD, (c) HP-γ-CD, (d) Pul, and (e–g) their nanofiber formulations, including (e) P4/HP-β-CD-loaded Pul fibers, (f) P4/HP-γ-CD-loaded Pul fibers, and (g) P4-loaded Pul fibers at (i) (0.5:1 - P4:CD).

Similar results were observed on the respective DTG curves of the samples (Figure 4.5). Thermal stability of P4 increased within the fibers. Likewise, the use of CDs boosted the thermal stability of the P4.

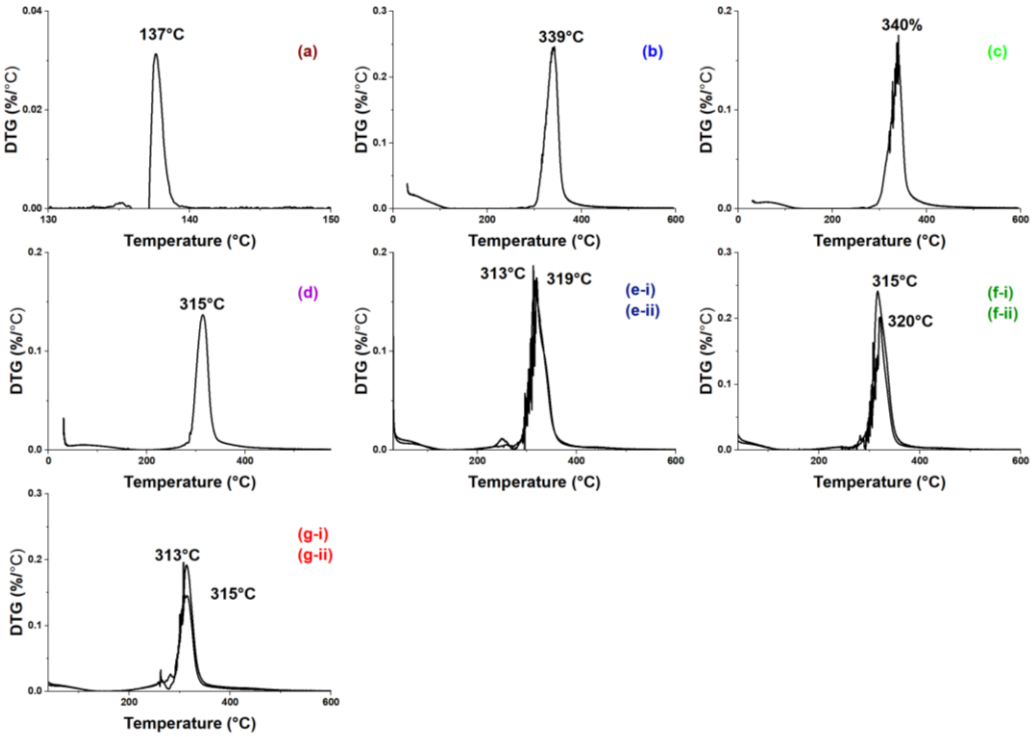

Figure 4.5: DTG curves of (a) pure P4, (b) HP-β-CD, (c) HP-γ-CD, (d) Pul, and (e–g) their nanofiber formulations, including (e) P4/HP-β-CD-loaded Pul fibers, (f) P4/HP-γ-CD-loaded Pul fibers, and (g) P4-loaded Pul fibers at (i) (0.5:1 - P4:CD) and (ii) (1:1 - P4:CD) molar ratios.

We performed dissolution tests to confirm that P4 formed ICs with both HP-β-CD and HP-γ-CD. P4 doesn't normally dissolve in water because it's hydrophobic. So, when the P4 dissolved from the fibers, it showed us that it had successfully formed complexes with the HP-β-CD and HP-γ-CD. From (Figure 4.6), we can see that these fibers with a 0.5:1 ratio of P4 to CD dissolved in water in about 60 seconds. But fibers with a 1:1 ratio didn't dissolve completely even after 90 seconds. This tells us that in the 1:1 ratio, there might be some P4/CD that didn't form complexes, which is why those particles didn't dissolve. As for the fibers without any CD, they barely dissolved even after 3 minutes of shaking the solution. This clearly highlights the critical role of cyclodextrins in enhancing the aqueous solubility of P4 by facilitating inclusion complex formation. It also suggests that using a lower P4-to-CD ratio ensures more efficient complexation, preventing the presence of unbound, hydrophobic P4 in the matrix. These results are consistent with the hypothesis that excess drug loading may lead to saturation of the CD cavity sites, limiting the formation of inclusion complexes.

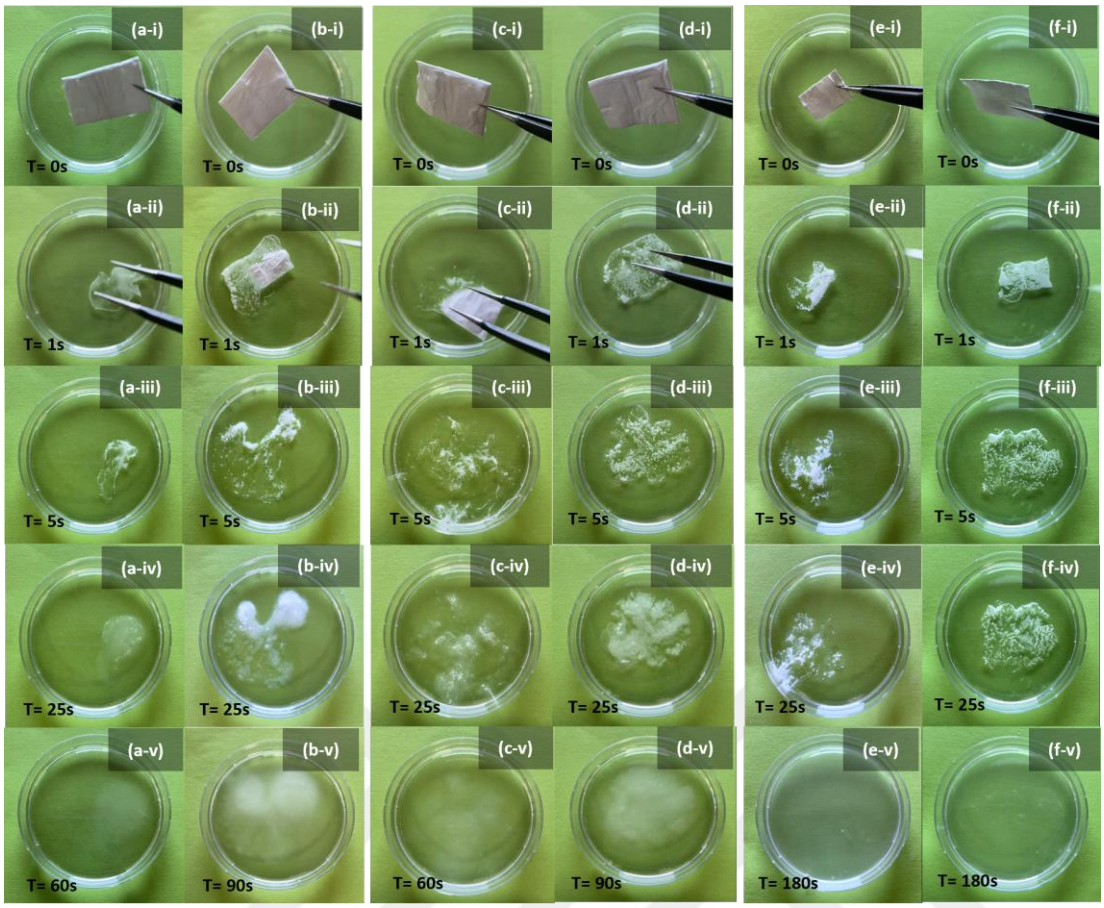

Figure 4.6: The progressive dissolution behavior of electrospun mats comprising of (a, b) Pul/P4/HP-β-CD IC, (c, d) Pul/P4/HP-γ-CD IC, (e, f) Pul/P4 at different drug: CD 0.5:1 (a, c, e) and 1:1 (b, d, f) stoichiometries in simulated saliva over time.

To see how the electrospun fibers would dissolve in a mouth-like setting, we placed them on tissues wetted with simulated saliva. Figure 4.7 shows that, similar to the previous dissolution tests, fibers containing either HP-β-CD or HP-γ-CD with a 0.5:1 P4: CD molar ratio dissolved quickly. However, those with a 1:1 ratio didn't fully dissolve even after a minute and the fibers without any CD dissolved much slower compared to the fibers that contained CD. The release of P4 from the fibers was followed through UV/vis spectroscopy (Figure 4.8). The results of UV/vis spectroscopy show that the sample containing HP-γ-CD exhibited the highest release of P4 (~50–55%). The HP-β-CD sample showed a moderate release (~35%). The CD-free sample demonstrated the lowest release (~25%). All release profiles reached a plateau within 20–30 minutes. For the fibers loaded with P4:CD (1:1), the sample containing HP-γ-CD exhibited the highest release (~25%). The HP-β-CD sample showed a comparable but slightly lower release (~20–25%). The CD-free sample

demonstrated the lowest release (~15%). The release profiles of all samples reached a plateau in 20–30 minutes.

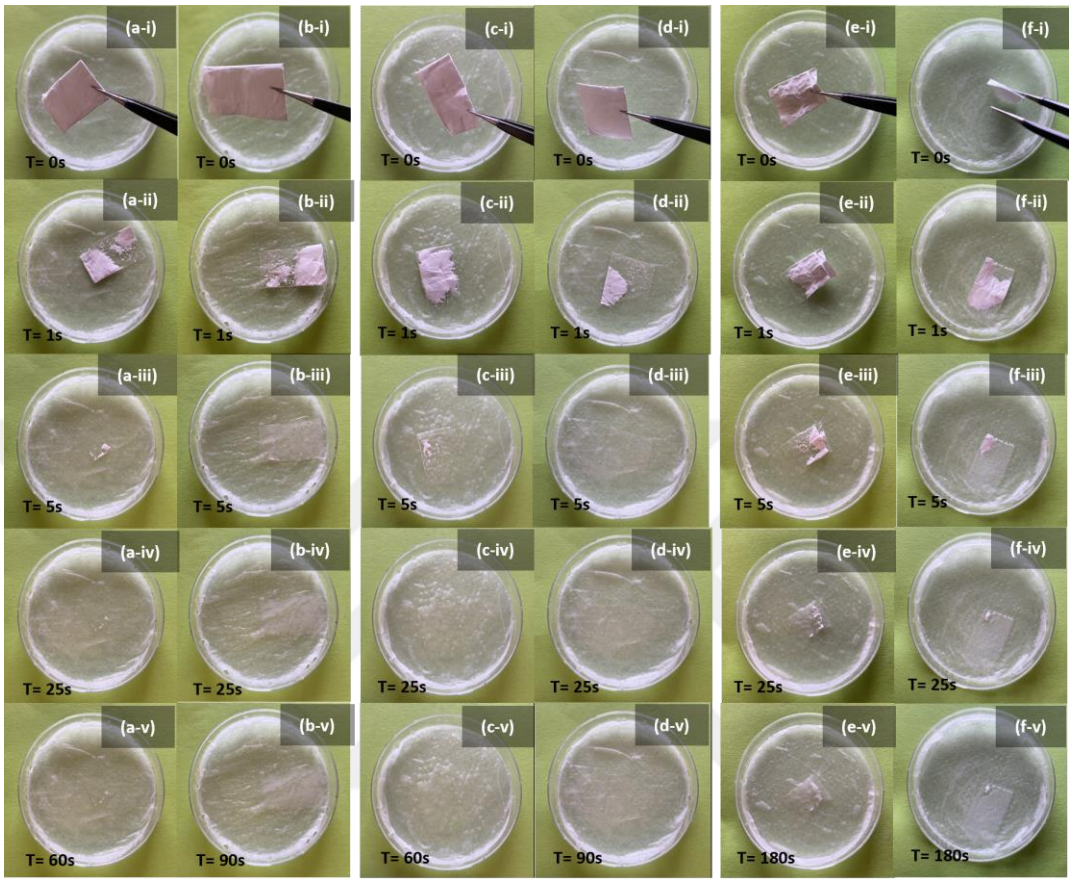

Figure 4.7: The progressive dissolution behavior of electrospun mats on tissues wetted with simulated saliva: (a, b) Pul/P4/HP-β-CD IC, (c, d) Pul/P4/HP-γ-CD IC, (e, f) Pul/P4 at different drug: CD 0.5:1 (a, c, e) and 1:1 (b, d, f) stoichiometries.

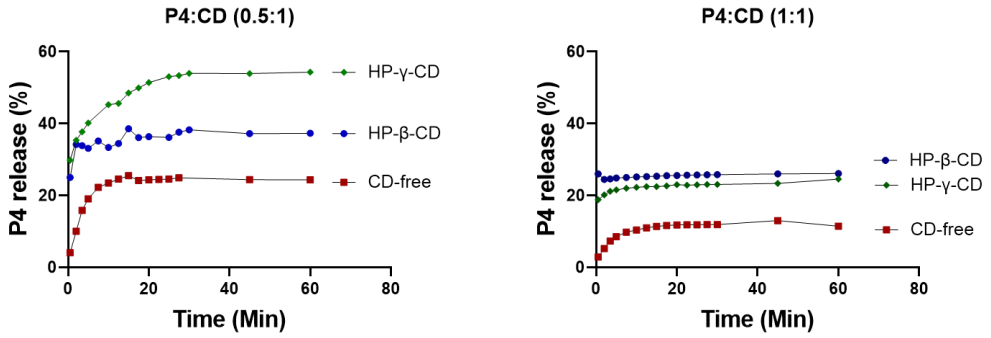

Figure 4.8: Time-dependent in-vitro release profiles of Pul/P4/HP-β-CD IC, Pul/P4/HP-γ-CD IC, and Pul/P4 fibers at different P4:CD (0.5:1 and 1:1) molar ratios.

4.1.2. Estradiol delivery

Similar to the observations with P4, all of the solutions exhibited a white, opaque appearance and the resulting fiber mats displayed desirable flexibility and mechanical strength. When working with E2, we found that reducing the concentration of HP-β-CD and HP-γ-CD from 20% w/v (used with P4) to 13% w/v resulted in thinner fibers. Similar to previous observations, a 1:1 E2: CD molar ratio produced thicker fibers with a more beaded appearance. In contrast, a 0.5:1 E2: CD molar ratio yielded smooth fibers without any beads. Fibers without any CD had the smallest diameters compared to those with either type of CD as Figure 4.9 demonstrates.

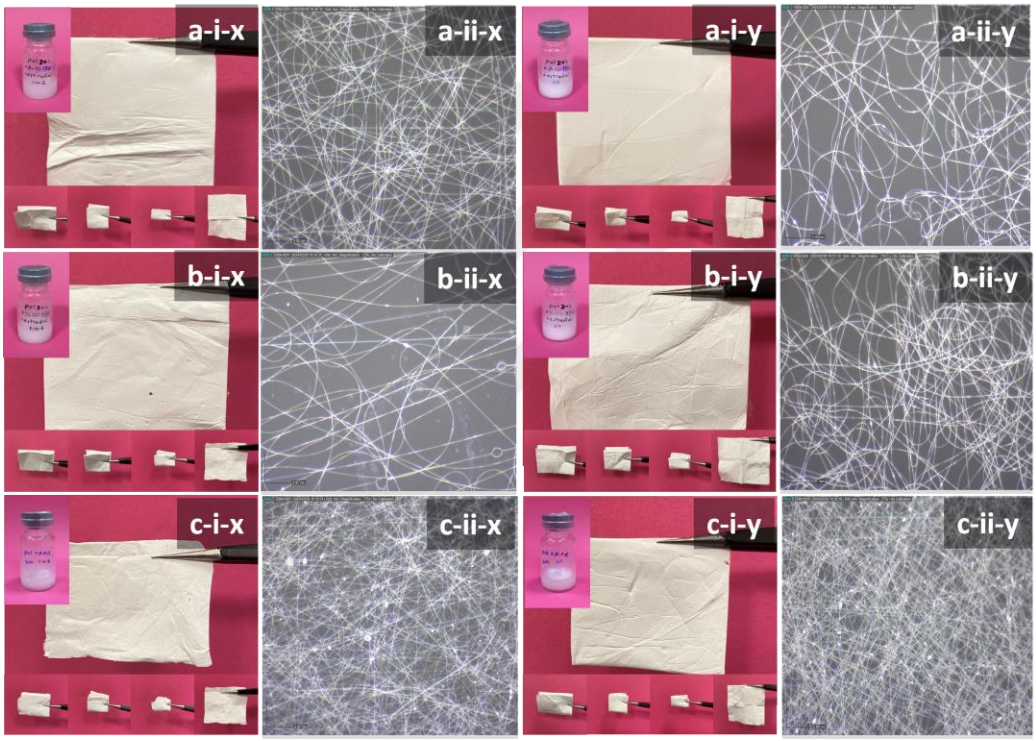

Figure 4.9: (i) Photos of electrospinning solutions, and electrospun nanofibers and (ii) microscopic images of (a) Pul/E2/HP-β-CD IC, (b) Pul/E2/HP-γ-CD IC, (c) Pul/E2 at different drug:CD (x) 0.5:1 and (y) 1:1 molar ratio.

Figure 4.10 presents SEM images of fibers produced using Pul/E2/HP-β-CD IC, Pul/E2/HP-γ-CD IC, and Pul/E2 at different drug-to-CD molar ratios: (i) 0.5:1 and (ii) 1:1. Regardless of the type of CD or the E2/CD molar ratio, all fibers exhibited a uniform bead-free structure. Increasing the drug content resulted in thicker fibers for both HP-β-CD and HP-γ-CD. In contrast, thinner fibers were observed in the absence of CD molecules (Figure 4.10c), likely due to the higher viscosity of solutions containing CD molecules.

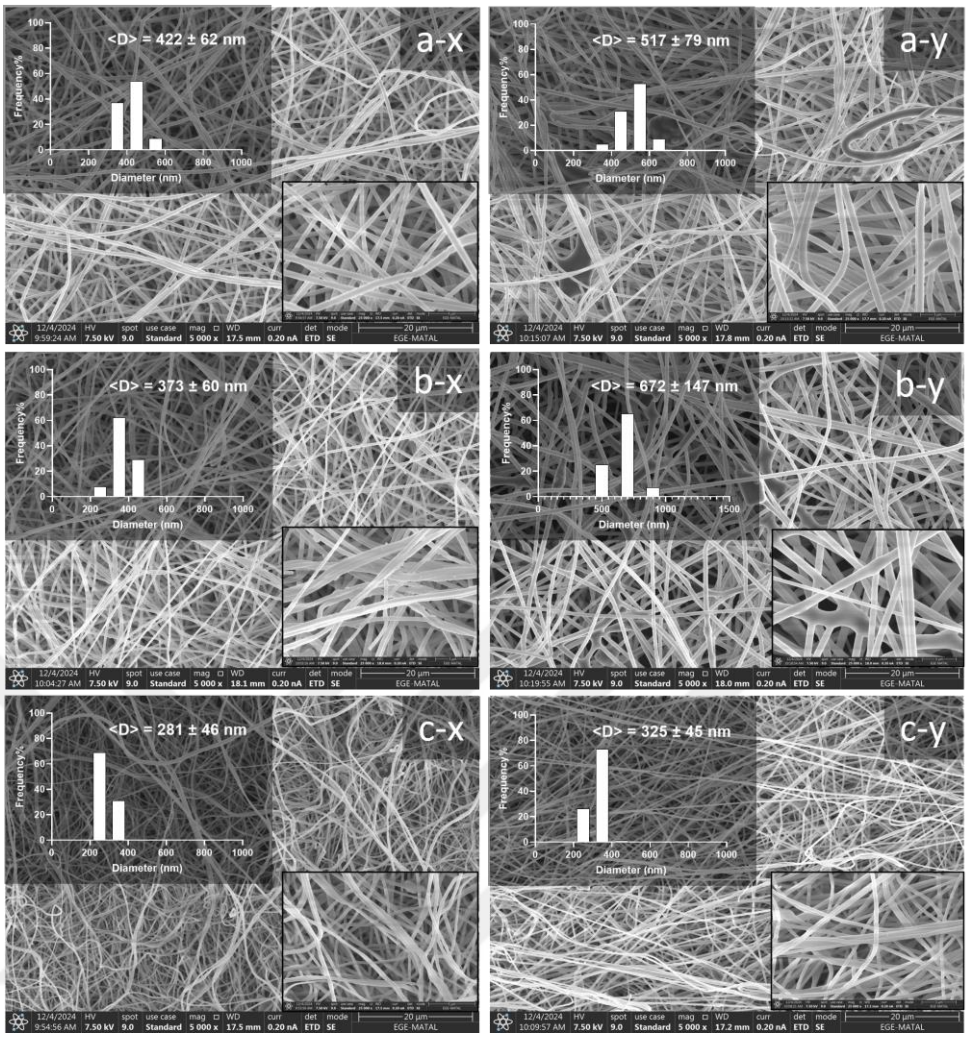

Figure 4.10: Scanning electron micrographs and diameter distribution histograms of (a) Pul/E2/HP-β-CD IC, (b) Pul/E2/HP-γ-CD IC, (c) Pul/E2 at different E2: HP-CD (x) 0.5:1 and (y) 1:1 stoichiometries.

The presence of E2 within fibers was confirmed by FTIR analyses. The fibers produced with two different molar ratios (0.5:1 and 1:1) and two different CDs were compared (Figure 4.11). The pure E2 spectrum shows distinctive sharp peaks in the 3000 cm^{-1} region and multiple peaks in the fingerprint region (1450–500 cm^{-1}). CDs (HP-β-CD and HP-γ-CD) maintain their characteristic broad peaks around 3400 cm^{-1} (O–H stretching) and distinctive peaks in the 1000–1200 cm^{-1} region (C–O stretching). The Pul spectrum remains consistent with the previous analysis, showing a broad peak around 3300 cm^{-1} and characteristic O-H stretching. In the ICs (Pul/E2/CD), the spectra exhibit features from both CD and E2, with notable changes in E2's characteristic peaks, suggesting successful IC formation. When comparing the 0.5:1

and 1:1 molar ratios, both demonstrate successful complex formation but with varying peak intensities.

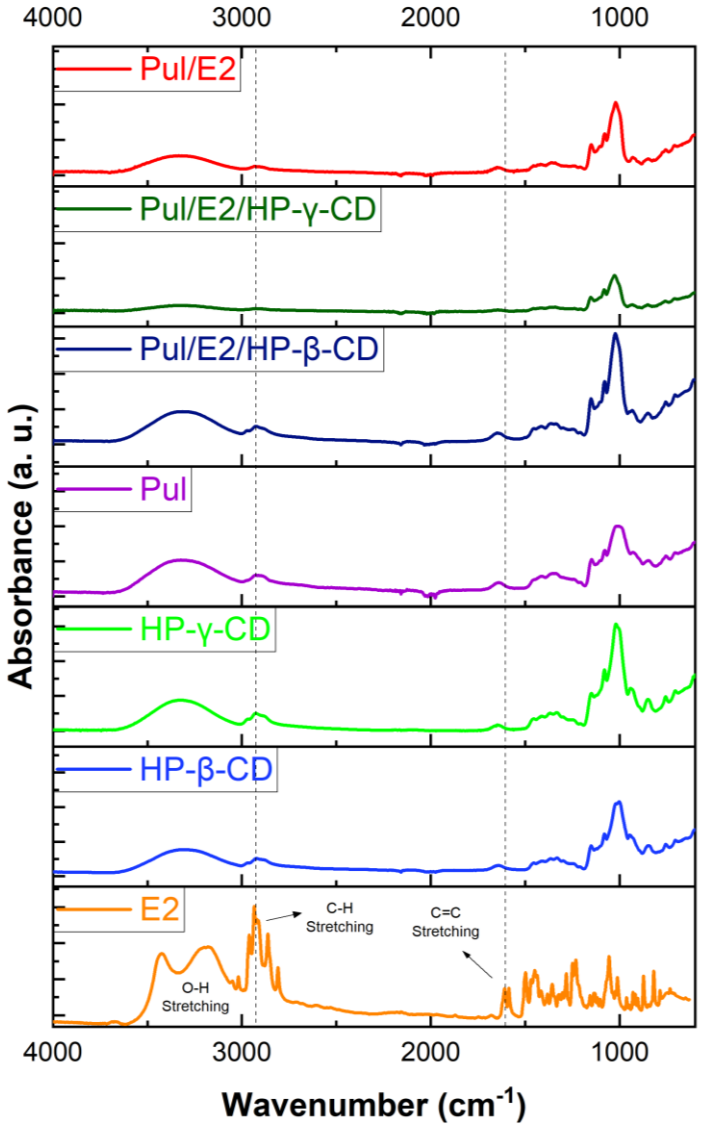

Figure 4.11: FTIR spectra presented from bottom to top: E2, HP-β-CD, HP-γ-CD, Pul, E2/HP-β-CD-loaded Pul fibers, E2/HP-γ-CD-loaded Pul fibers, and E2-loaded Pul fibers at a (0.5:1 - E2:CD molar ratio).

The thermal stability of E2-loaded fibers was analyzed (Figures 4.12 & 4.13). E2 exhibited two decomposition patterns: the first mass loss resulted from the loss of water molecules, while the second, occurring below 200 °C, corresponded to the decomposition of E2. In contrast, both CDs (HP-β-CD and HP-γ-CD) decomposed above 290 °C but displayed a mass loss below 150 °C due to the loss of adsorbed water. Pul, like the CDs, demonstrated thermal stability, decomposing above 280 °C.

Notably, in E2-loaded fibers, the thermal stability of E2 was enhanced. However, in the absence of CDs, the thermal stability of E2 decreased.

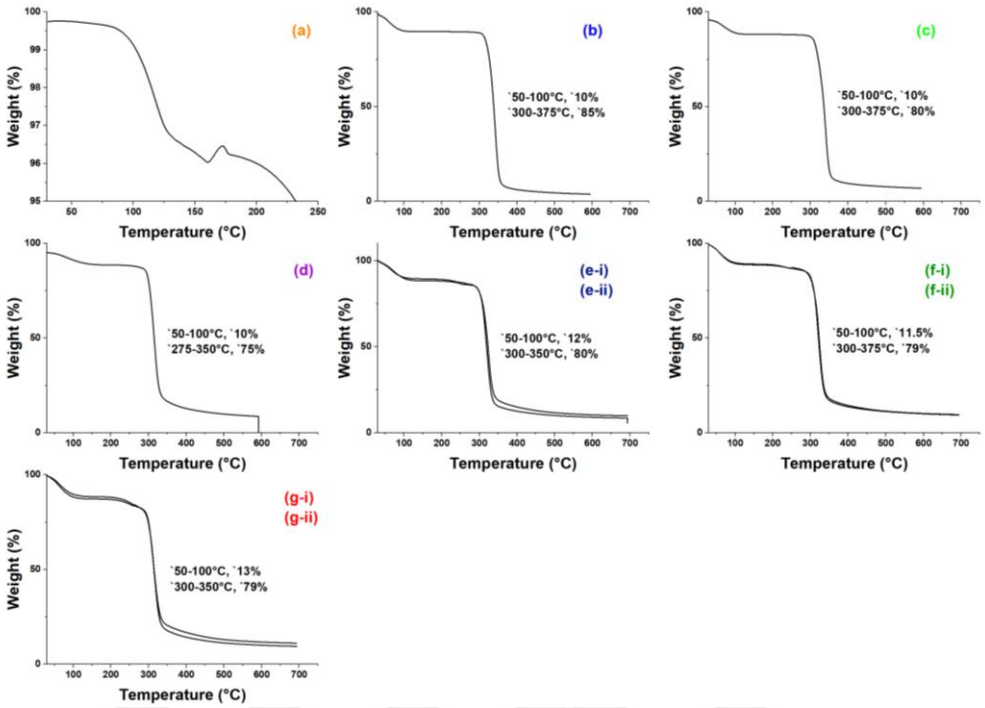

Figure 4.12: The thermogravimetric analysis of pure (a) E2, (b) HP-β-CD, (c) HP-γ-CD, (d) Pul, and (e–g) their nanofiber formulations, including (e) E2/HP-β-CD-loaded Pul fibers, (f) E2/HP-γ-CD-loaded Pul fibers, and (g) E2-loaded Pul fibers at i. (0.5:1 - P4:CD) and ii. (1:1 - P4: CD) molar ratios.

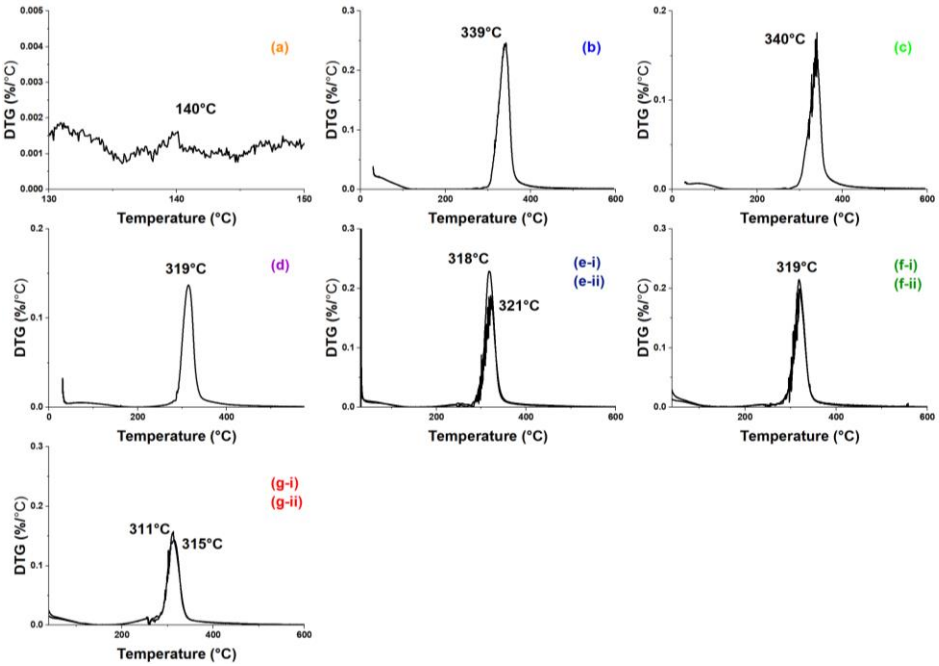

Figure 4.13: DTG curves of pure E2, HP-β-CD, HP-γ-CD, Pul, and their nanofiber formulations, including E2/HP-β-CD-loaded Pul NFs, E2/HP-γ-CD-loaded Pul NFs, and E2-loaded Pul NFs at (a) 0.5:1 (E2:CD) and (b) 1:1 (E2:CD) molar ratios.

Figure 4.14 shows the dissolution behavior of different fiber types. Clearly the fibers with a 0.5:1 E2: CD ratio dissolved rapidly in water, within 60 seconds. Notably, fibers containing HP-β-CD dissolved slightly faster than those with HP-γ-CD, suggesting a potential advantage in terms of dissolution rate. This quick dissolution suggests the successful formation of E2/CD ICs. On the other hand, fibers with a 1:1 ratio exhibited incomplete dissolution even after 75 seconds. This observation implies that not all E2/CD formed ICs at this ratio, leaving some undissolved particles. Lastly, the CD-free fibers showed minimal dissolution even after 3 minutes of shaking, highlighting the significant role of CD in enhancing E2's solubility.

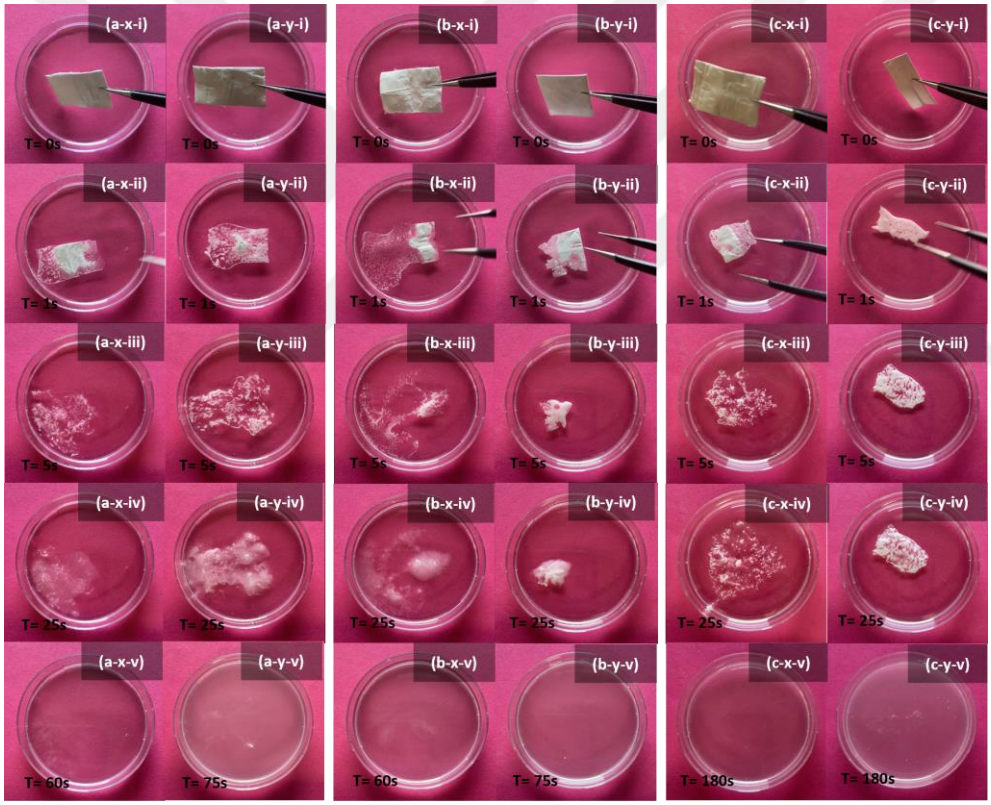

Figure 4.14: The progressive dissolution behavior of electrospun mats comprising of (a) Pul/E2/HP-β-CD IC, (b) Pul/E2/HP-γ-CD IC, (c) Pul/E2 at different drug:CD (x) 0.5:1 and (y) 1:1 stoichiometries in simulated saliva over time.

To see how the electrospun fibers would dissolve in a mouth-like setting, we placed them on tissues wetted with simulated saliva (Figure 4.15). Similar to the previous dissolution tests, fibers containing either HP-β-CD or HP-γ-CD with a 0.5:1 E2: CD molar ratio dissolved quickly. However, those with a 1:1 ratio didn't fully dissolve

even after a minute. The fibers without any CD dissolved much slower compared to the fibers that contained CD.

The release of E2 from the fibers exhibited a burst release, with a significant portion of E2 being released within the first 5 minutes, followed by a slower release. A similar pattern was observed for fibers produced at a 1:1 molar ratio. Due to the higher drug content in these fibers, a greater percentage of drug release was observed (Figure 4.16).

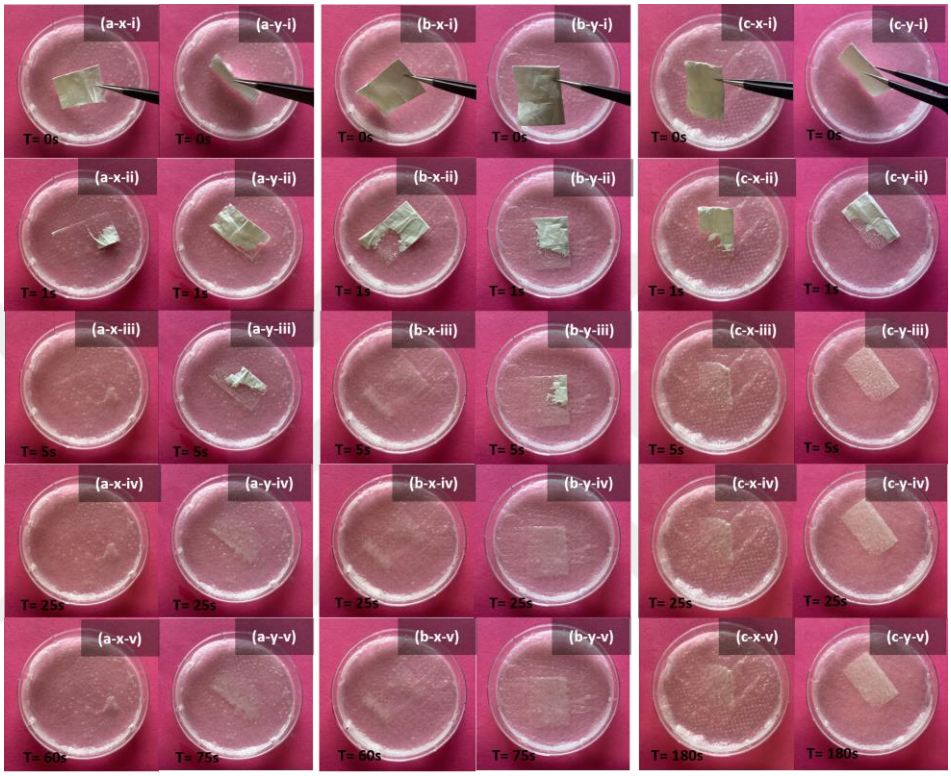

Figure 4.15: The progressive dissolution behavior of electrospun mats on tissues wetted with simulated saliva. (a) Pul/E2/HP-β-CD IC, (b) Pul/E2/HP-γ-CD IC, (c) Pul/E2 at different drug: CD (x) 0.5:1 and (y) 1:1 stoichiometries in simulated saliva over time.

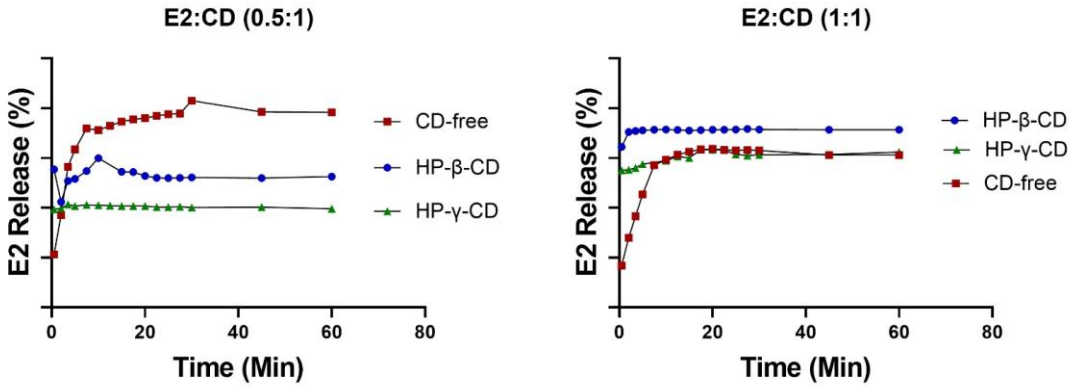

Figure 4.16: Time-dependent in-vitro release profile of Pul/E2/HP-β-CD IC, Pul/E2/HP-γ-CD IC, and Pul/E2 at different drug:CD (0.5:1 and 1:1) stoichiometries.

4.1.3. Estriol delivery

The E3-loaded fiber solutions consistently exhibited a white, opaque appearance, and the resulting electrospun mats displayed favorable flexibility and mechanical strength (Figure 4.17). Incorporating either HP-β-CD or HP-γ-CD generally yielded thicker fibers with minimal beading. However, a 1:1 E3: CD molar ratio resulted in fibers with a higher incidence of beading and larger diameters compared to those produced using a 0.5:1 E3: CD molar ratio.

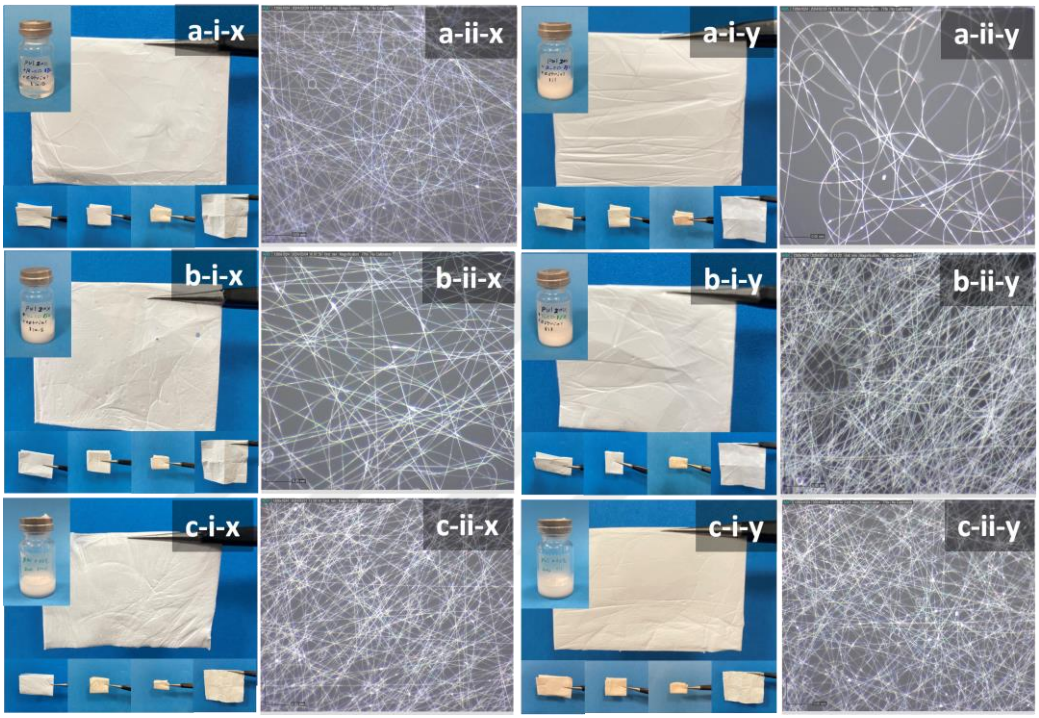

Figure 4.17: (i) Photos of electrospinning solutions, and electrospun nanofibers and (ii) Digital microscopic images of (a) Pul/E3/HP-β-CD IC, (b) Pul/E3/HP-γ-CD IC, (c) Pul/E3 at different drug:CD (x) 0.5:1 and (y) 1:1 stoichiometries.

Similar to previous observations with P4 and E2 hormones, the CD-free nanofibers exhibited smaller diameters and a more pronounced beaded morphology compared to their CD-containing counterparts, as illustrated in Figure 4.18. This suggests that the presence of cyclodextrins plays a significant role in modulating fiber morphology during electrospinning. Specifically, the mean fiber diameters of pullulan nanofibers loaded with E3/HP-β-CD complexes at 0.5:1 and 1:1 molar ratios were measured as 510 ± 51 nm and 555 ± 62 nm, respectively. In contrast, the corresponding values for the fibers incorporating HP-γ-CD were 312 ± 58 nm and 278 ± 55 nm, respectively, indicating finer fibers with this particular CD. Meanwhile, the pullulan nanofibers

containing the same amounts of E3 but without any CD inclusion showed even smaller average diameters of 274 ± 51 nm and 308 ± 51 nm for the same molar ratios. These findings clearly demonstrate the thickening effect of HP-β-CD on fiber formation, likely due to its stronger interaction with the drug and the polymer matrix, which influences the viscosity and electrospinnability of the solution.

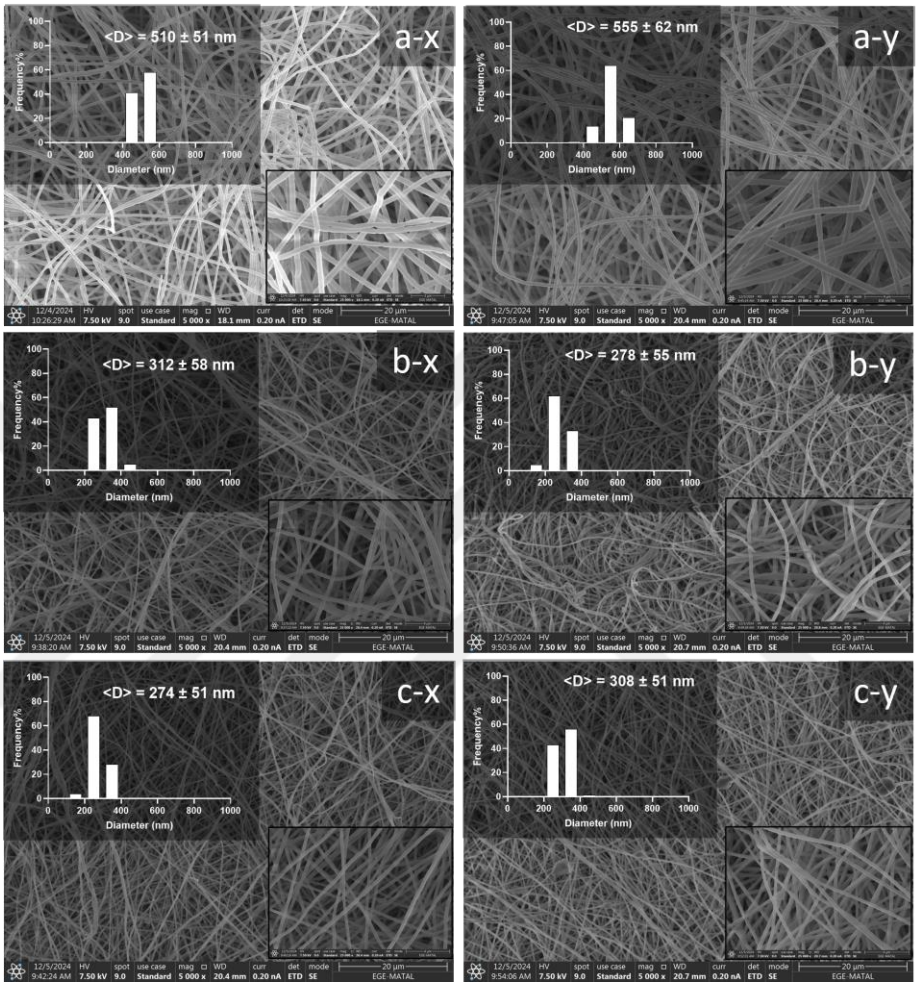

Figure 4.18: Scanning electron micrographs and diameter distribution histograms of (a) Pul/E3/HP-β-CD IC, (b) Pul/E3/HP-γ-CD IC, (c) Pul/E3 at different E3:HP-CD (x) 0.5:1 and (y) 1:1 stoichiometries.

The FTIR spectra show a compositional analysis of E3 ICs with pullulan and CDs (Figure 4.19). The pure E3 spectrum displays distinctive features with multiple sharp peaks in the fingerprint region (1450–500 cm^{-1}), C=C stretching at ~1650 cm^{-1} and C-H stretching in the region of ~2800–3000 cm^{-1}, reflecting its unique steroidal structure. The CD spectra (HP-β-CD and HP-γ-CD) maintain their characteristic broad hydroxyl stretching bands near 3400 cm^{-1} and typical saccharide-related peaks in the lower wavenumber region. The Pul/E3/CD fibers show a shoulder at ~1610 cm^{-1} due to C=C

stretching. The Pul matrix, characterized by its broad hydroxyl band and polysaccharide peaks, appears to successfully incorporate the E3-CD complexes.

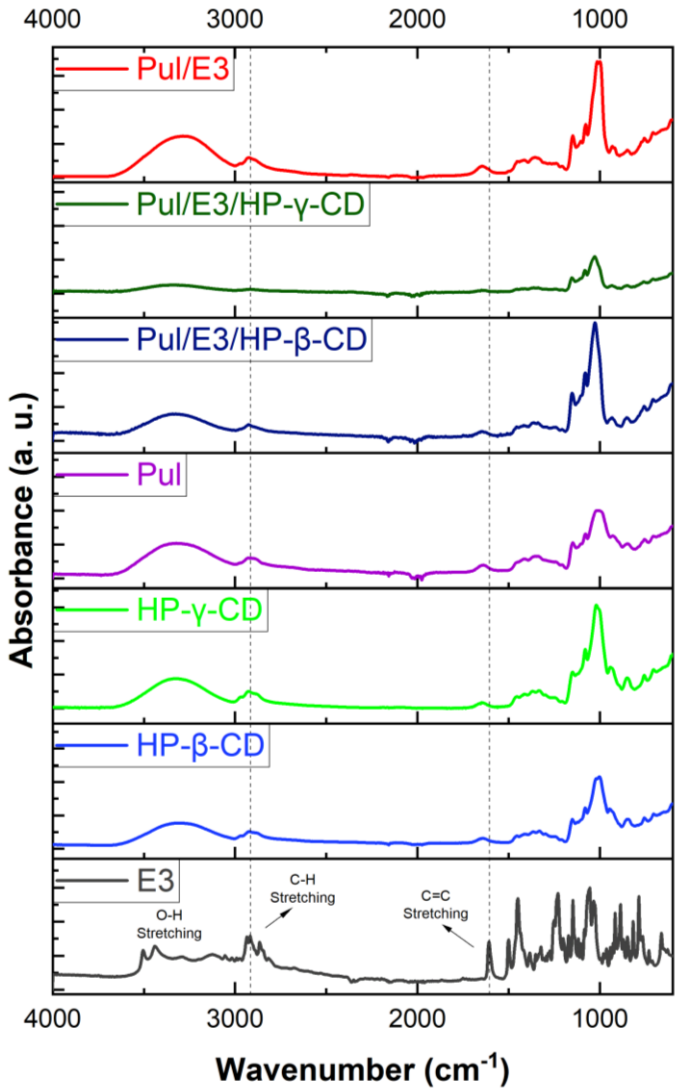

Figure 4.19: FTIR spectra presented from bottom to top: E3, HP-β-CD, HP-γ-CD, Pul, E3/HP-β-CD-Loaded Pul NFs, E3/HP-γ-CD-Loaded Pul NFs, and E3-loaded Pul NFs at a (0.5:1 - E2:CD molar ratio).

The thermal stability of E3 was evaluated using TGA, which demonstrated a distinct mass loss beginning at approximately 150°C (Figure 4.20). In contrast, both HP-β-CD and HP-γ-CD exhibited excellent thermal stability, with decomposition initiating only at temperatures around 300°C. For the E3-loaded fibers, a slight mass loss was observed starting from 200°C, indicating that the incorporation of E3 into the fiber matrix contributes to its stabilization.

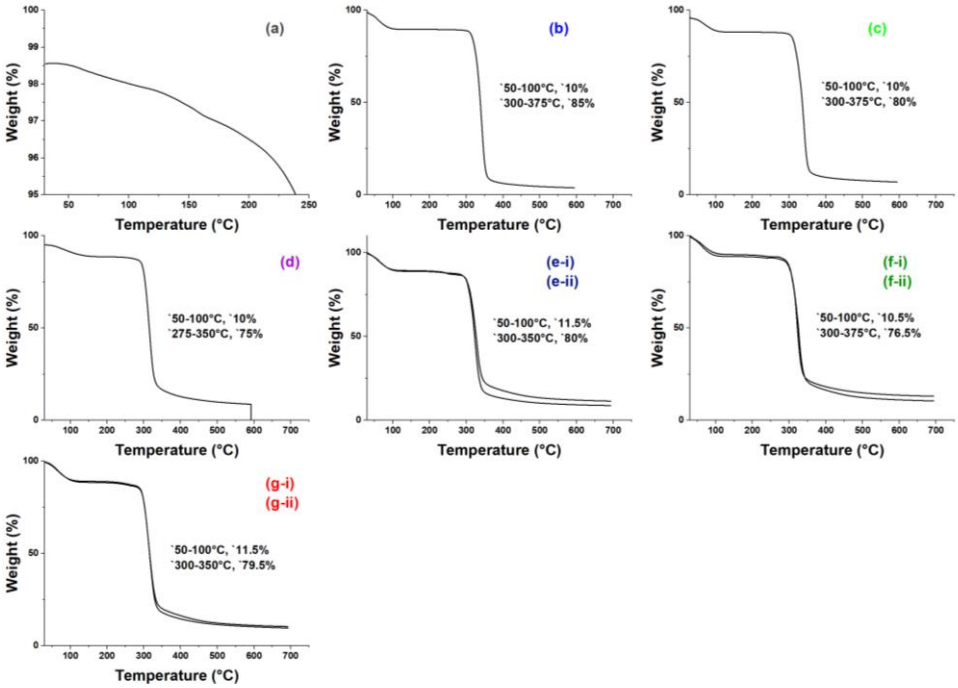

Figure 4.20: The thermogravimetric analysis of pure E3, HP-β-CD, HP-γ-CD, Pul, and their nanofiber formulations, including E3/HP-β-CD-loaded Pul NFs, E3/HP-γ-CD-loaded Pul NFs, and E3-loaded Pul NFs at a. (0.5:1 – E3:CD) and b. (1:1 – E3:CD) molar ratios.

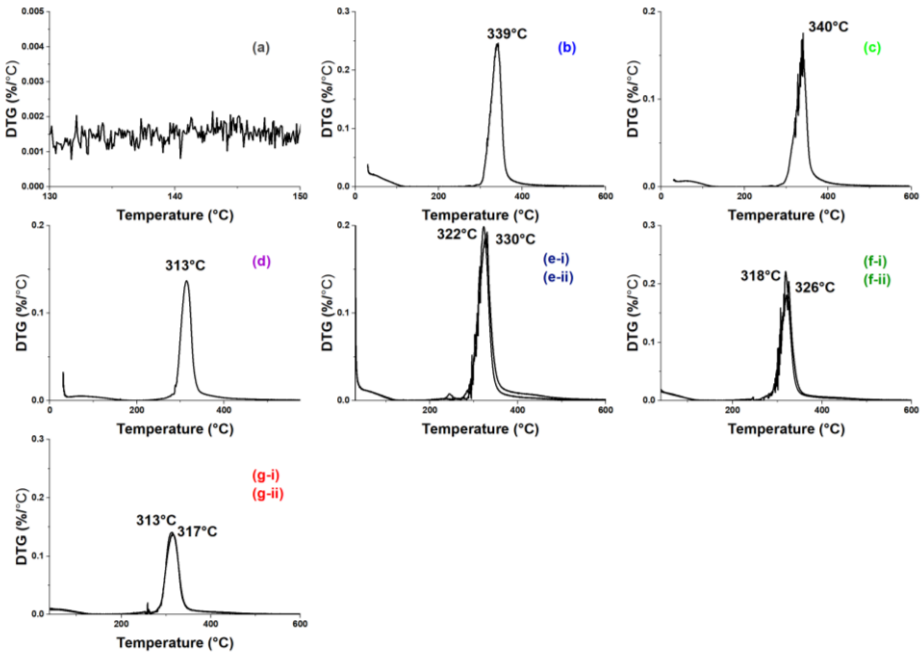

Figure 4.21: DTG curves of pure E3, HP-β-CD, HP-γ-CD, Pul, and their nanofiber formulations, including E3/HP-β-CD-loaded Pul NFs, E3/HP-γ-CD-loaded Pul NFs, and E3-loaded Pul NFs at a. (0.5:1 E3-CD) and b. (1:1 – E3:CD) molar ratios.

A similar trend was evident in DTG curves (Figure 4.21), where the onset of mass loss for E3-loaded fibers occurred at a lower temperature compared to pure CDs, further supporting the stabilization effect. The differences in thermal degradation profiles between pure E3, the CD complexes, and the fiber-loaded systems highlight the influence of the fiber matrix on the thermal properties of the encapsulated compound. Figure 4.22 illustrates the dissolution behavior of E3-loaded nanofibers. Electrospun fibers containing a 0.5:1 E3: HP-β-CD molar ratio exhibited the fastest dissolution, dissolving completely within approximately 60 seconds. Fibers with a 0.5:1 estriol: HP-γ-CD molar ratio dissolved slightly slower, requiring around 80 seconds for complete dissolution. Notably, both HP-β-CD and HP-γ-CD-containing fibers with a 0.5:1 E3: CD molar ratio dissolved significantly faster than their counterparts with a 1:1 E3: CD molar ratio. The latter exhibited incomplete dissolution even after 90 seconds, suggesting the presence of free E3 molecules that did not form ICs with the CDs. As expected, CD-free nanofibers showed the lowest solubility, remaining undissolved even after 3 minutes. This observation underscores the crucial role of CDs in enhancing the solubility of hydrophobic hormones like E3.

In order to test the dissolution in an oral environment, the fiber mats were placed on tissues wetted with simulated saliva (Figure 4.23). Similar to the aqueous dissolution studies, fibers containing either HP-β-CD or HP-γ-CD with an E3:CD molar ratio of 0.5:1 dissolved rapidly. However, with a ratio of 1:1, incomplete dissolution was observed after more than one minute. At both molar ratios, the dissolution of HP-β-CD containing fibers was slightly higher compared to those with HP-γ-CD. As expected, fibers without CDs dissolved to a far lesser extent compared with the ones containing CDs, thus underlining the role of CDs in rendering E3 readily soluble within a simulated oral environment. These observations reinforce the importance of optimizing the CD content to avoid uncomplexed E3, which can hinder the dissolution efficiency in physiological conditions. The faster dissolution seen with HP-β-CD may be attributed to its better affinity for E3, possibly due to its cavity size or molecular compatibility. Moreover, this behavior suggests that HP-β-CD may be the more suitable carrier for oral formulations aiming for rapid onset of action. Ultimately, the results support the potential of CD-loaded nanofibers as an effective platform for delivering poorly soluble drugs like E3 via the oral mucosa.

Figure 4.22: The progressive dissolution behavior of electrospun mats comprising of (a) Pul/E3/HP-β-CD IC, (b) Pul/E3/HP-γ-CD IC, (c) Pul/E3 at different drug:CD (x) 0.5:1 and (y) 1:1 stoichiometries in simulated saliva over time.

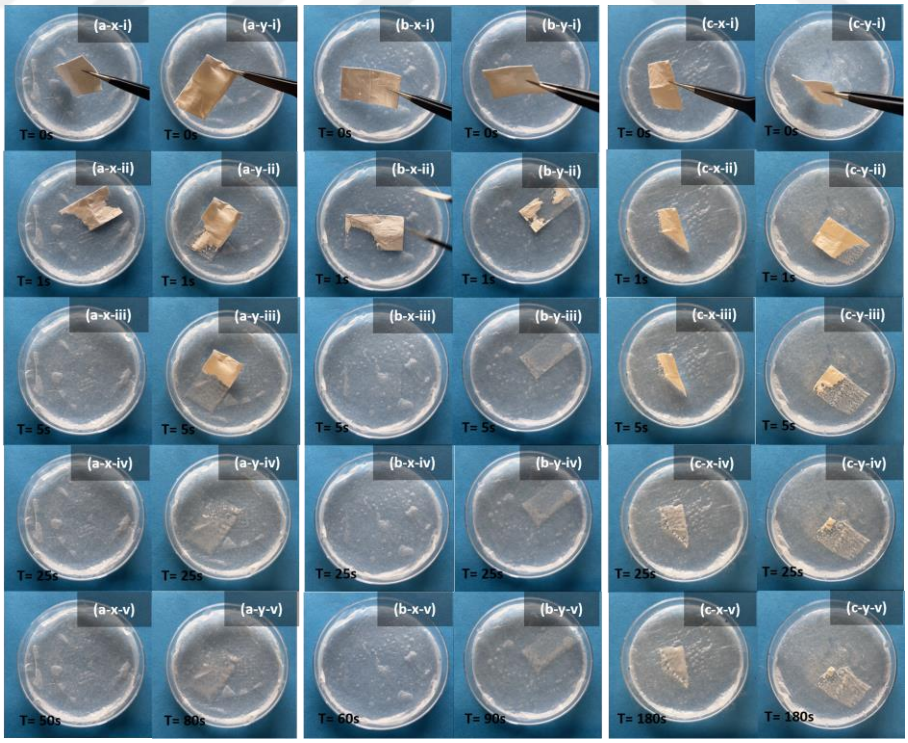

Figure 4.23: The progressive dissolution behavior of electrospun mats comprising of (a) Pul/E3/HP-β-CD IC, (b) Pul/E3/HP-γ-CD IC, (c) Pul/E3 at different drug: CD (x) 0.5:1 and (y) 1:1 stoichiometries when placed on simulated saliva-moistened tissues.

The in-vitro release study of E3 from Pul fibers revealed distinct release patterns based on CD complexation and stoichiometry (Figure 4.24). When examining the 0.5:1 drug:CD ratio, the CD-free formulation demonstrated the highest release rate, achieving approximately 90% release after 60 minutes, while formulations containing CD complexes showed more controlled release patterns. Specifically, the HP-γ-CD complex exhibited an intermediate release of around 55%, and the HP-β-CD complex showed the lowest release at about 35%. When the drug:CD ratio was increased to 1:1, the release profiles of all formulations became more similar, with final release percentages converging between 60–70%. All formulations at this ratio reached their plateau within 20 minutes, with the HP-γ-CD complex showing a slightly higher initial release rate. The initial release kinetics were rapid in the first 10 minutes for all formulations, followed by a plateau phase. These findings demonstrate that CD complexation can effectively modulate estriol release from pullulan fibers, with both the type of CD and the stoichiometry ratio playing crucial roles in controlling the release behavior in aqueous conditions.

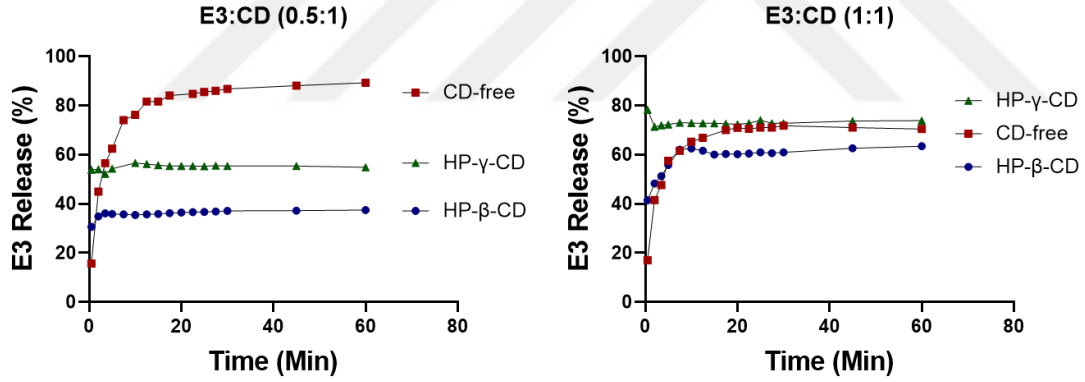

Figure 4.24: Time-dependent in-vitro release profile of Pul/E3/HP-β-CD IC, Pul/E3/HP-γ-CD IC, and Pul/E3 at different E3: CD (0.5:1 and 1:1) stoichiometries.

These results suggest that precise tuning of the drug-to-CD ratio is essential for balancing sustained release with desired therapeutic levels. Furthermore, the ability of HP-β-CD to produce a more prolonged release profile highlights its potential for applications requiring extended drug availability, while HP-γ-CD may be more suitable for faster onset formulations. Overall, the study confirms that pullulan-based electrospun fibers, when combined with cyclodextrins, represent a versatile and tunable platform for the delivery of hydrophobic drugs like E3.

4.2 Cellulose Acetate/Gelatin/Cellulose Acetate Sandwich Nanofibrous Films for Hormone Delivery

4.2.1. Progesterone delivery

Figure 4.25 shows that the outer layer solutions, composed of CA, exhibited high viscosity and transparency. In contrast, the middle layer solutions, consisting of Gel/P4 with either HP-β-CD, HP-γ-CD, or no CD, were opaque. Notably, the Gel solutions containing either type of CD (HP-β-CD or HP-γ-CD) were more viscous than the CD-free solution. The added CD molecules increased the solution's viscosity. Despite the varying properties of these layers, the resulting sandwich mats demonstrated flexibility and foldability. Even after being folded three times, no signs of brittleness were observed. Microscopic examination revealed distinct differences in fiber morphology between the layers. The hydrophobic CA outer layers displayed thick, highly beaded

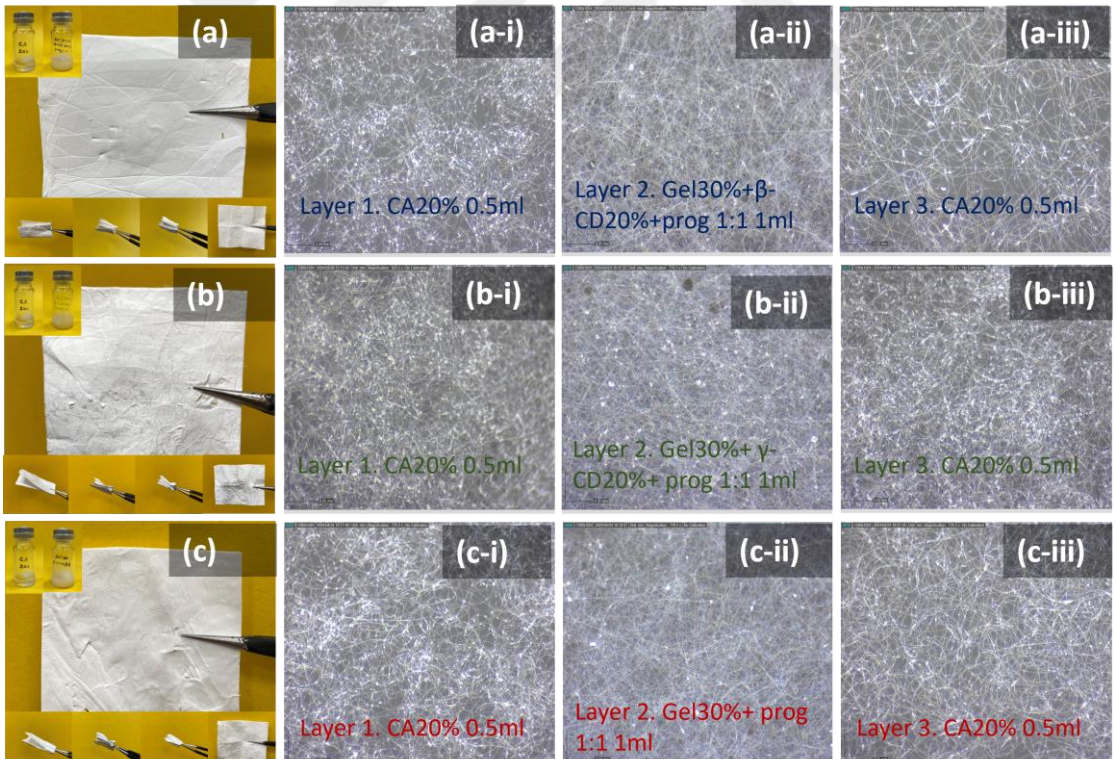

Figure 4.25: Optical photos of electrospinning solutions and electrospun mats, and microscopic images of sandwich fibers of CA+ Gel/P4+ CA with (a) HP-β-CD IC, (b) HP-γ-CD IC and (c) CD-free at 1:1 stoichiometry. (i) First layer, (ii) second layer and (iii) third layer.

nanofibers (Figure 4.25). The Gel middle layers also exhibited beaded fibers but were thinner compared to the CA fibers.

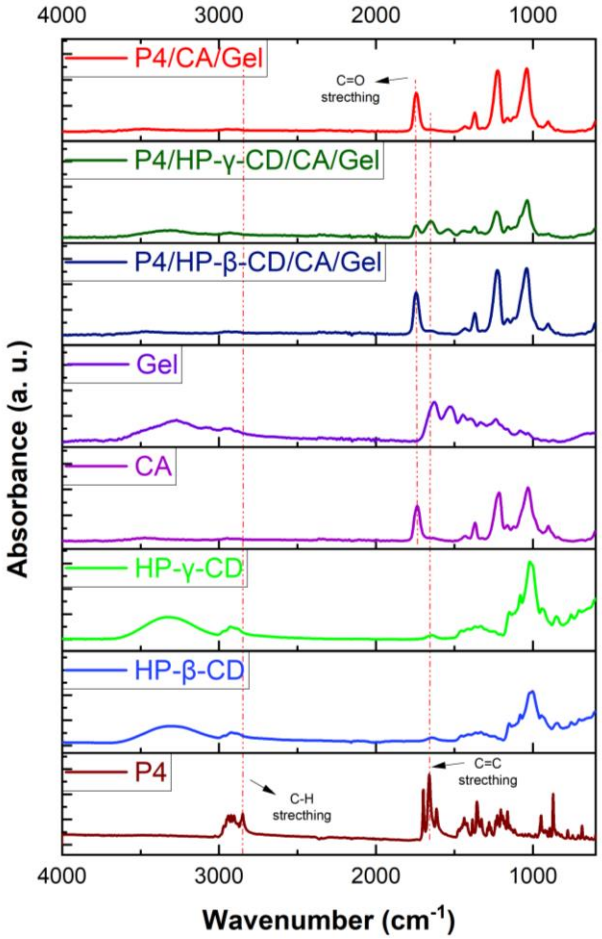

Figure 4.26: FTIR spectra presented from bottom to top: P4, HP-β-CD, HP-γ-CD, CA, Gel, P4/HP-β-CD-loaded CA-Gel-CA NFs, P4/HP-γ-CD-loaded CA-Gel-CA NFs, and P4-loaded CA-Gel-CA NFs at a (1:1 - P4:CD molar ratio).

The FTIR spectra provide comprehensive evidence of successful incorporation of P4 into a multilayered fiber system composed of CA and Gel layers, with and without CD ICs (Figure 4.26). The characteristic peaks corresponding to the carbonyl stretching vibrations of the ketone groups at C_3 and C_{20} for P4 are observed at 1661 cm^{-1} and 1693 cm^{-1}, respectively, distinguishing P4 from other steroids (Benoit vd., 1986). The CDs (HP-β-CD and HP-γ-CD) show their typical broad hydroxyl bands around 3400 cm^{-1} and characteristic peaks in the lower frequency region. CA also displays distinctive peaks in the respective range, while the Gel spectrum shows its characteristic peaks between 1615 and 1620 cm^{-1} which be assigned to intermolecular β-sheet. In the final multilayered structures (P4/CA/Gel and P4/HP-CD/CA/Gel), the

spectra demonstrate features from all components, with some modifications in peak intensities and positions, particularly in the C=O stretching region. The presence of CDs in the P4/HP-β-CD/CA/Gel and P4/HP-γ-CD/CA/Gel samples appears to influence the overall spectral profile, suggesting successful IC formation within the multilayered fiber structure. These spectral changes confirm the successful integration of P4, either directly or as CD complexes, into the CA-Gel multilayered fiber system. Figure 4.27 presents the TGA analysis of multilayered fiber films loaded with P4. The P4 exhibited a single-stage decomposition between 150°C and 250°C, indicating lower thermal stability. In contrast, HP-β-CD and HP-γ-CD decomposed between 300°C and 350°C, corresponding to the breakdown of glucopyranose rings, with HP-γ-CD displaying slightly higher thermal stability. Water loss, observed between 50°C and 120°C, is attributed to moisture from Gel and CDs. Notably, the P4/CD-loaded systems demonstrated greater thermal stability than the P4/CD-free system, emphasizing the protective effect of molecular encapsulation on P4's thermal degradation (Figure 4.27). The incorporation of P4 with HP-β-CD and HP-γ-CD in the three-layered nanofibers successfully inhibited P4's characteristic decomposition peak. It is important to note that the P4 content in the sandwich fibers is minimal, making its decomposition challenging to detect.

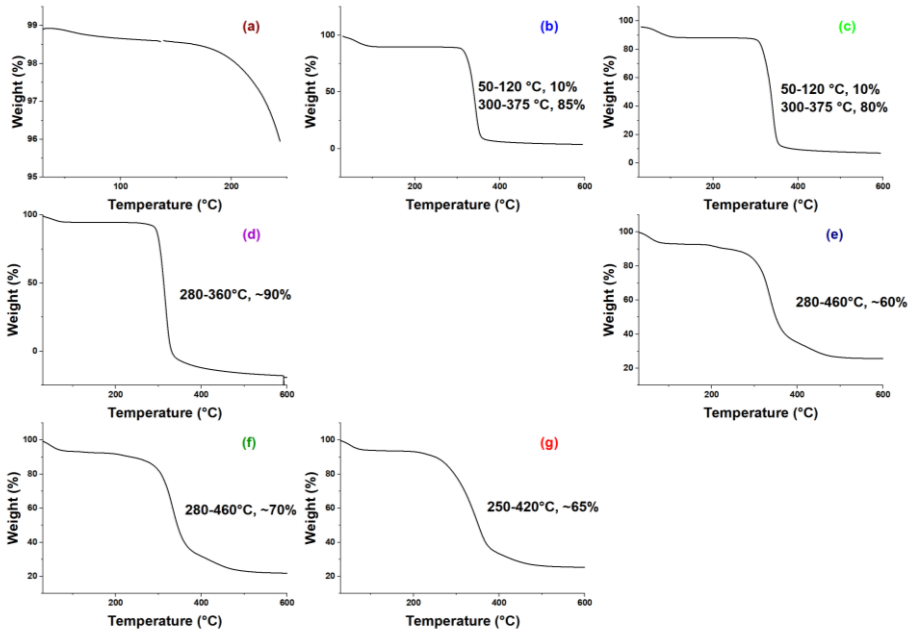

Figure 4.27: The thermogravimetric analysis of (a) P4, (b) HP-β-CD, (c) HP-γ-CD, (c) CA, (d) Gel, (e) P4/HP-β-CD-loaded CA/Gel/CA tri-layered NFs, (f) P4/HP-γ-CD-loaded CA/Gel/CA 3 layered NFs, and (g) P4-loaded CA/Gel/CA 3 layered NFs at a (1:1 - P4:CD molar ratio).

The dissolution tests in Figure 4.28 reveal that these tri-layered sandwich-structured nanofiber mats did not dissolve in simulated saliva. This was due to the hydrophobic CA outer layers. Compared with the quickly dissolved Gel fibers, CA layers led to insoluble mats in water-based simulated saliva and maintained the whole shape and structure of these mats. While the mats containing either type of CD had already partially dissolved within 3 seconds, the CD-free mats did not dissolve even after 900 seconds. This therefore indicated the important role of CDs in enhancing the solubility of P4. When placed on tissue moistened with simulated saliva, the fibers containing either type of HP-CD in their inner layers exhibited partial disintegration within 60 seconds (Figure 4.28). In contrast, the fibers without HP-CDs did not dissolve even after 15 minutes.

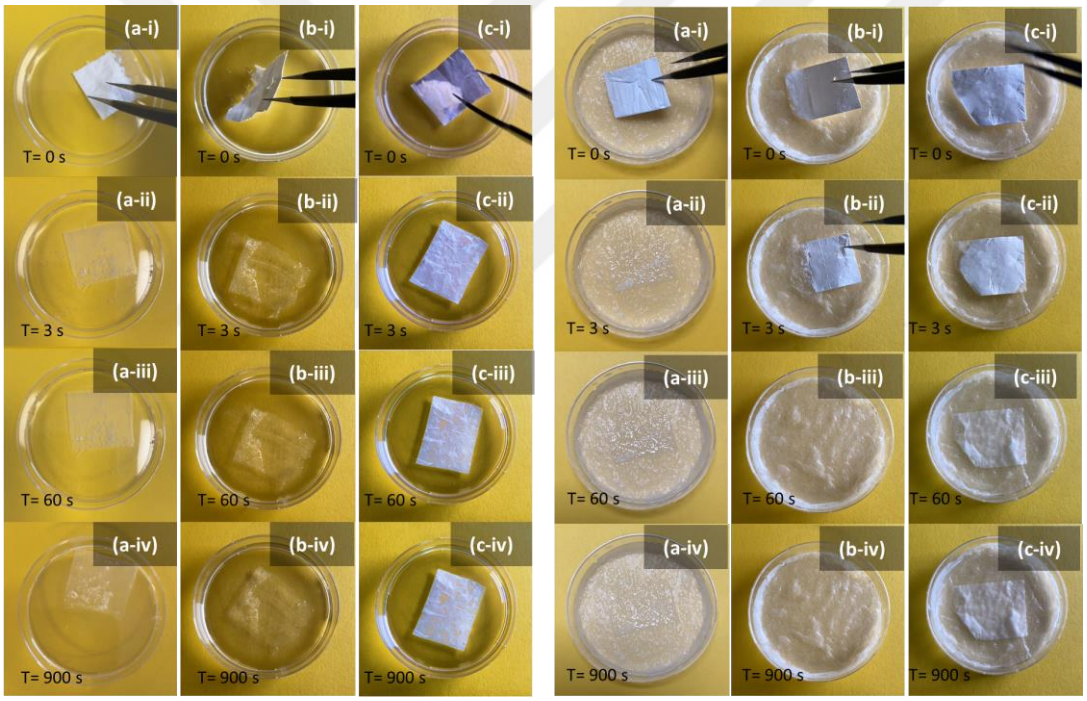

Figure 4.28: (Left panel) The progressive dissolution behavior of tri-layered electrospun mats comprising of CA as outer layers and Gel/P4 incorporated with (a) HP-β-CD, (b) HP-γ-CD and (c) CD-free at 1:1 stoichiometry as the inner layer, in simulated saliva over time. (Right panel) The progressive dissolution behavior of tri-layered electrospun mats comprising of CA as outer layers and Gel/P4 incorporated with (a) HP-β-CD, (b) HP-γ-CD and (c) CD-free at 1:1 stoichiometry as the inner layer, when placed on simulated saliva-moistened tissues.

The UV-Vis analysis presented in Figure 4.29 underscores the critical role of HP-β-CD and HP-γ-CD in modulating P4 release from the tri-layered sandwich nanofibers. Fibers loaded with HP-β-CD exhibited a rapid initial release of P4, whereas those

containing HP-γ-CD demonstrated a slower and more sustained release profile, indicative of stronger interactions between HP-γ-CD and P4 within the IC. These findings illustrate that the choice of CDs significantly influences the release kinetics of P4, HP-γ-CD providing a more controlled and therapeutically advantageous release compared to HP-β-CD or the absence of CDs.

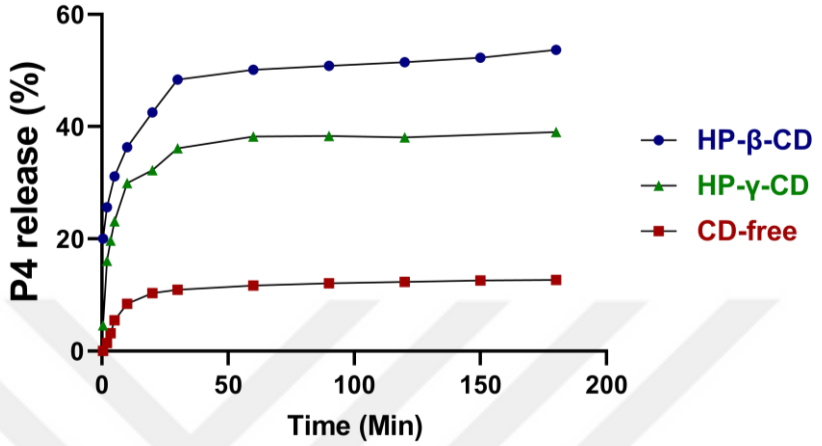

Figure 4.29: Time-dependent in-vitro release profile of tri-layered electrospun mats comprising of CA as outer layers and Gel/P4 incorporated with (a) HP-β-CD, (b) HP-γ-CD and (c) CD-free at 1:1 stoichiometry as the inner layer.

4.2.2. Estradiol delivery

The release of the E2 hormone was studied using a tri-layered nanofiber structure similar to the P4 delivery system. All formulations containing Gel, E2, and either HP-β-CD, HP-γ-CD, or no CD were opaque, and the resulting electrospun nanofibers exhibited favorable mechanical qualities, such as flexibility and foldability. Microscopic examination showed that the outer layer fibers were irregularly shaped and had noticeable beading. In contrast, the fibers in the inner layer, which included either HP-β-CD or HP-γ-CD, were more consistent, thinner, and had less beading. Inner layer fibers without CDs were the thinnest but exhibited more beading, as shown in Figure 4.30. These morphological differences suggest that the presence of CDs, particularly HP-β-CD and HP-γ-CD, contributes to enhanced fiber uniformity and improved electrospinning stability. The reduced beading in CD-containing fibers may be attributed to increased solution viscosity and improved electrostatic interactions during fiber formation, which support more continuous jet flow.

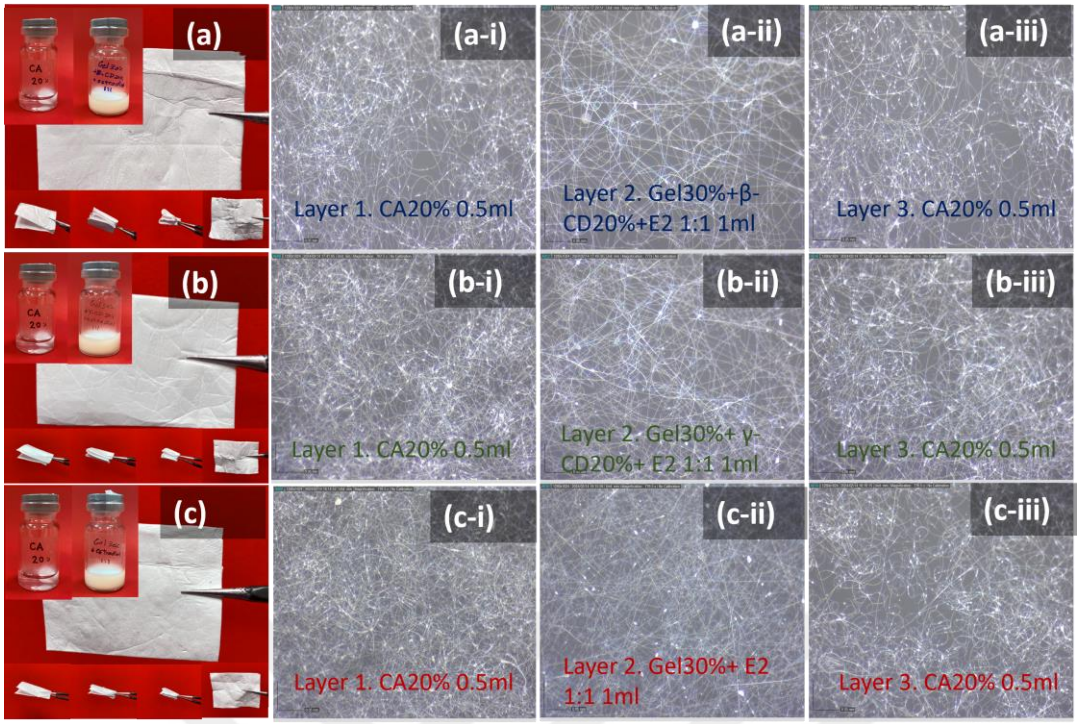

Figure 4.30: Optical photos of electrospinning solutions, electrospun nanofibers and microscopic images of CA+ Gel/ E2+ CA with (a) HP-β-CD IC, (b) HP-γ-CD IC and (c) CD-free at 1:1 stoichiometry. (i) first layer, (ii) second layer and (iii) third layer.

The FTIR spectra demonstrate the successful incorporation of E2 into a multilayered fiber system consisting of CA and Gel layers, both with and without CD ICs (Figure 4.31). The pure E2 spectrum shows its characteristic peaks, with distinctive C-H stretching bands around 3000 cm^{-1}, aromatic C=C stretching at ~1630 cm^{-1}, and C-H bending peak in the fingerprint region. CDs (HP-β-CD and HP-γ-CD) maintain their characteristic broad hydroxyl bands around 3400 cm^{-1}. CA exhibits its characteristic peaks that are preserved in the composite structures, while the Gel spectrum shows typical amide bands. In the multilayered structures (E2/CA/Gel and E2/HP-CD/CA/Gel), the spectra reveal features from all components, with noticeable modifications in peak intensities and positions. The incorporation of CDs in the E2/HP-β-CD/CA/Gel and E2/HP-γ-CD/CA/Gel samples influences the overall spectral profile, indicating effective IC formation within the multilayered fiber structure. These spectral shifts, particularly in the fingerprint region and near the hydroxyl and carbonyl bands, suggest strong intermolecular interactions between E2, CDs, and the polymer matrix.

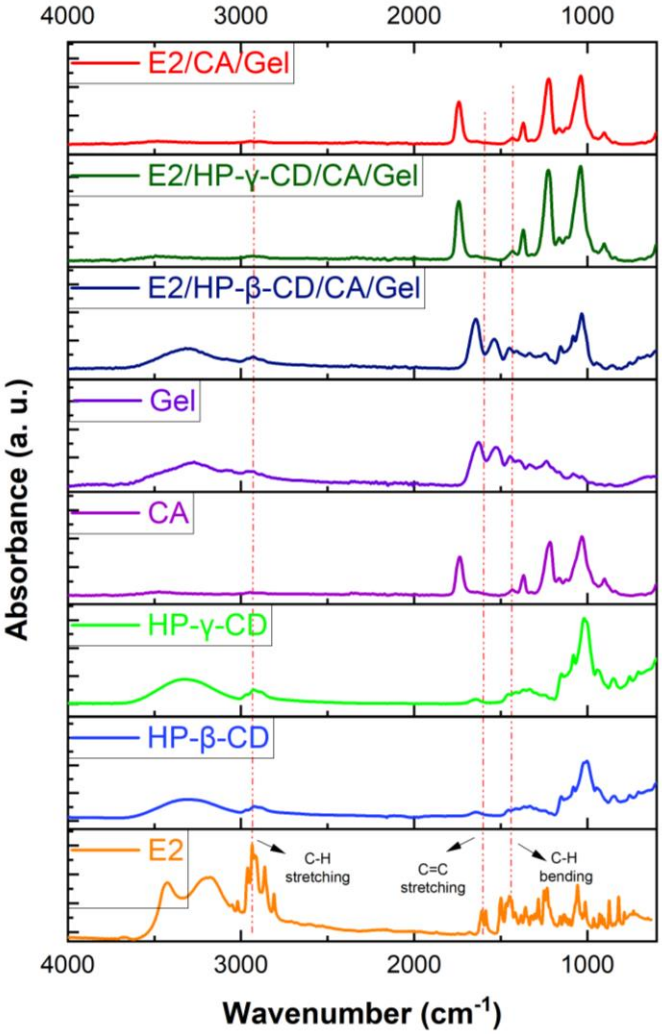

Figure 4.31: FTIR spectra presented from bottom to top: E2, HP-β-CD, HP-γ-CD, CA, Gel, E2/HP-β-CD-loaded CA-Gel-CA NFs, E2/HP-γ-CD-loaded CA-Gel-CA NFs, and E2-loaded CA-Gel-CA NFs at a (1:1 - E2:CD molar ratio).

The thermal stability of the E2-loaded fibers was assessed using TGA (Figure 4.32). Similar to P4, E2 began to degrade at approximately 200°C, with the initial mass loss attributed to water evaporation. In contrast, both HP-β-CD and HP-γ-CD molecules showed thermal stability, starting to decompose around 300°C. Due to the lower drug content in the sandwich fibers, no significant change in the thermal stability of E2 was detected. This suggests that the encapsulation of E2 within the multilayered fiber matrix does not compromise the thermal integrity of the overall system, making it suitable for processing and storage under standard conditions.

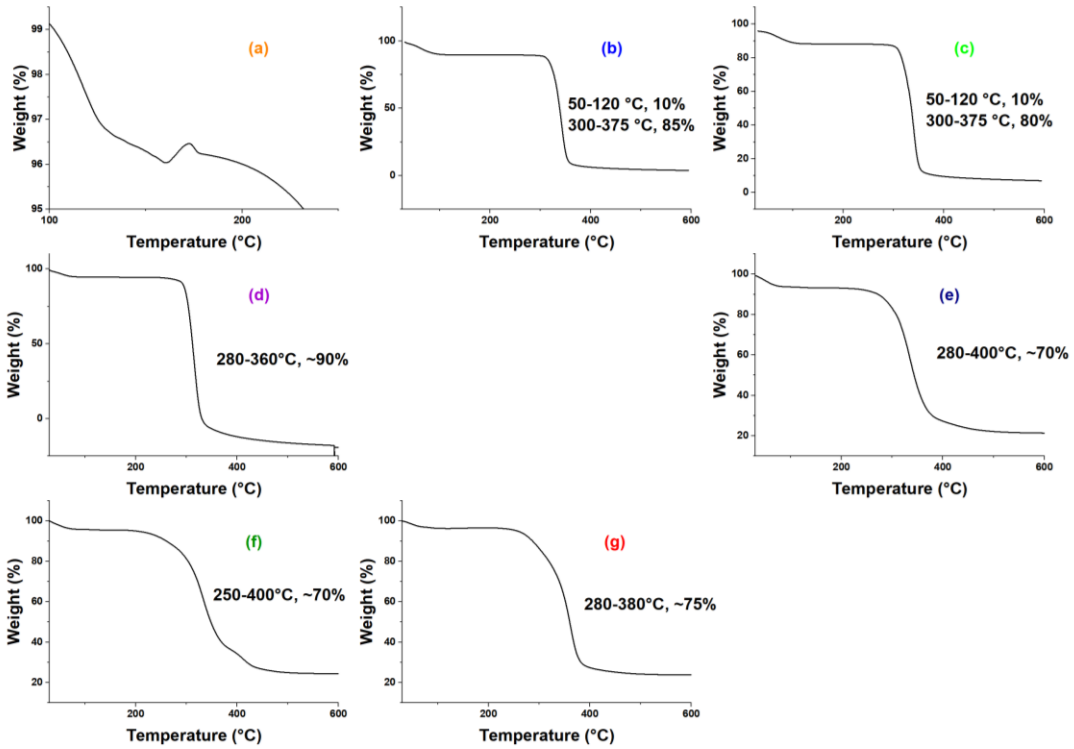

Figure 4.32: The thermogravimetric analysis of E2, HP- β -CD, HP- γ -CD, CA, gelatin, E2/HP-β-CD-loaded CA/Gel/CA tri-layered NFs, E2/HP-γ-CD-loaded CA/Gel/CA 3 layered NFs, and E2-loaded CA/Gel/CA 3 layered NFs at a (1:1 E2-CD molar ratio).

As presented in Figure 4.33 (left panel), dissolution studies were performed and reported, indicating that no formulations of the E2-loaded fibers, with or without the presence of HP-β-CD or HP-γ-CD, exhibited measurable dissolution in simulated saliva, even for an extended duration of 15 minutes. This excellent stability is attributed to the presence of the hydrophobic CA outer layer that protects the encapsulated drug from the aqueous environment. To more accurately reflect physiological conditions in the oral cavity, the fibers were then laid on tissues pre-saturated with simulated saliva (Figure 4.33, right panel). Similar to the observation before, all three types of fibers remained intact after 15 minutes. These results in total strongly indicate that such a tri-layered fiber system, especially its mechanically robust CA outer layer, could be a novel way to develop systems for controlled and sustained release of E2 other than traditional oral administration.

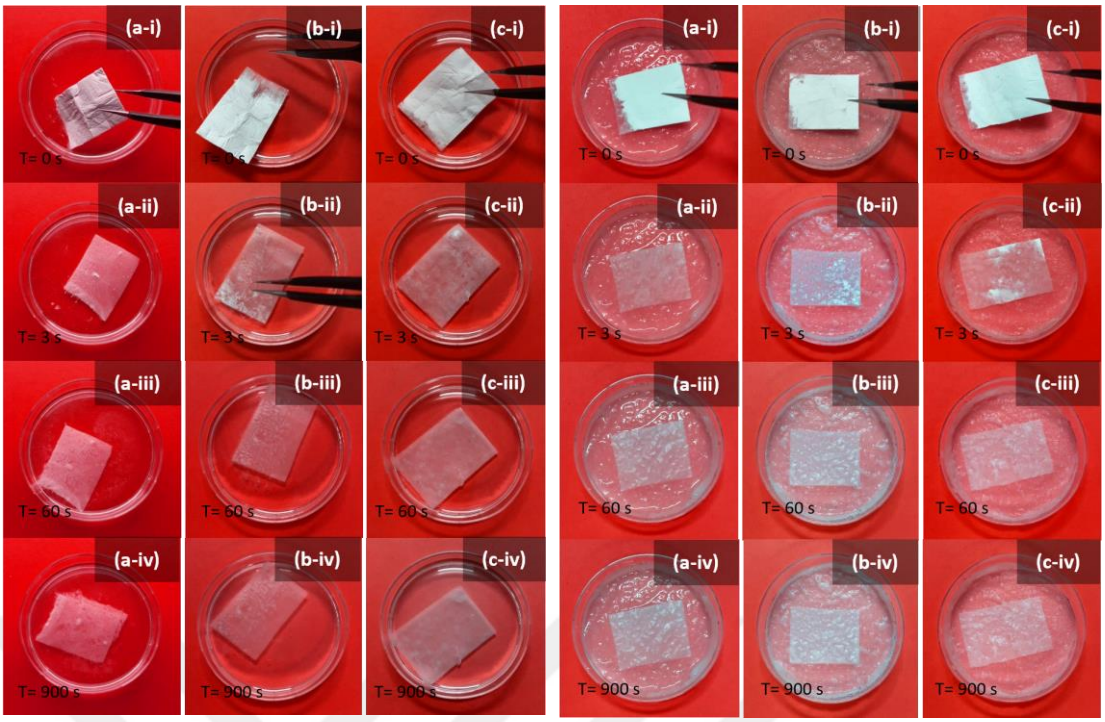

Figure 4.33: (Left panel) The progressive dissolution behavior of tri-layered electrospun mats comprising of CA as outer layers and Gel/P4 incorporated with (a) HP-β-CD, (b) HP-γ-CD and (c) CD-free at 1:1 stoichiometry as the inner layer, in simulated saliva over time. (Right panel) The progressive dissolution behavior of tri-layered electrospun mats comprising of CA as outer layers and Gel/P4 incorporated with (a) HP-β-CD, (b) HP-γ-CD and (c) CD-free at 1:1 stoichiometry as the inner layer, when placed on simulated saliva-moistened tissues.

UV analysis of the tri-layered nanofiber system (CA outer layers and inner layer of Gel/E2 with different formulations of CD) presents various profiles of release for E2. (Figure 4.34). Formulation with HP-β-CD shows controlled and sustained release of E2 over time. The release profile indicates that the HP-β-CD acts on the moderation of release rates, showing during the time of measurement a higher level of concentration of E2. Similar to the results found for the HP-β-CD formulation, a sustained release was obtained with HP-γ-CD; however, the obtained concentrations of E2 are slightly lower. This may suggest that HP-γ-CD is also an extremely effective complexing agent in prolonging the release, but less so compared to HP-β-CD. CD-free formulation is characterized by a rapid initial release of E2, followed by its quicker decline in concentration. Therefore, this indicates a less controlled release of the drug, hence making the formulation not that suitable for prolonged delivery purposes.

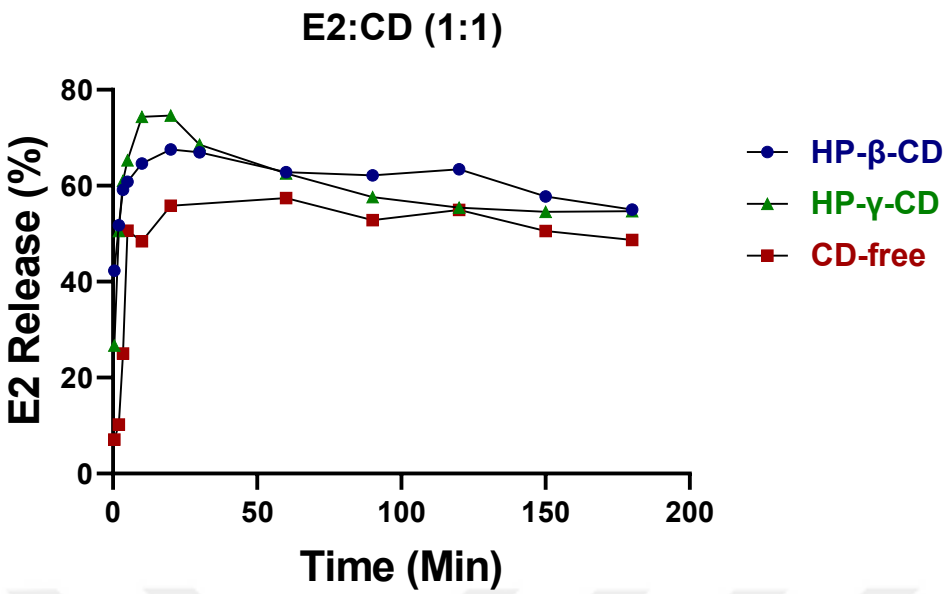

Figure 4.34: Time-dependent in-vitro release profile of tri-layered electrospun mats comprising of CA as outer layers and Gel/E2 incorporated with (a) HP-β-CD, (b) HP-γ-CD and (c) CD-free at 1:1 stoichiometry as the inner layer.

4.2.3. Estriol delivery

A similar approach was applied to investigate E3 delivery, with the concentration of CA in the outer layer solution increased to 25% w/v for its relevance. Fibers produced using this higher CA concentration exhibited a smoother morphology with reduced bead formation compared to fibers made with a 20% w/v CA solution. This improvement is likely due to the increased viscosity of the spinning solution. The electrospun fibers demonstrated excellent mechanical properties, including high flexibility and strength. Microscopic analysis revealed that the addition of either HP-β-CD or HP-γ-CD to the inner layer resulted in fibers with smooth morphologies and reduced beading compared to fibers without CD (Figure 4.35). These observations suggest that optimizing the polymer concentration in the outer layer, along with CD incorporation in the inner layer, plays a key role in achieving uniform fiber morphology and enhancing electrospinning stability. The presence of CDs not only improves fiber formation but also contributes to better drug dispersion within the matrix, potentially leading to more predictable and sustained release profiles.

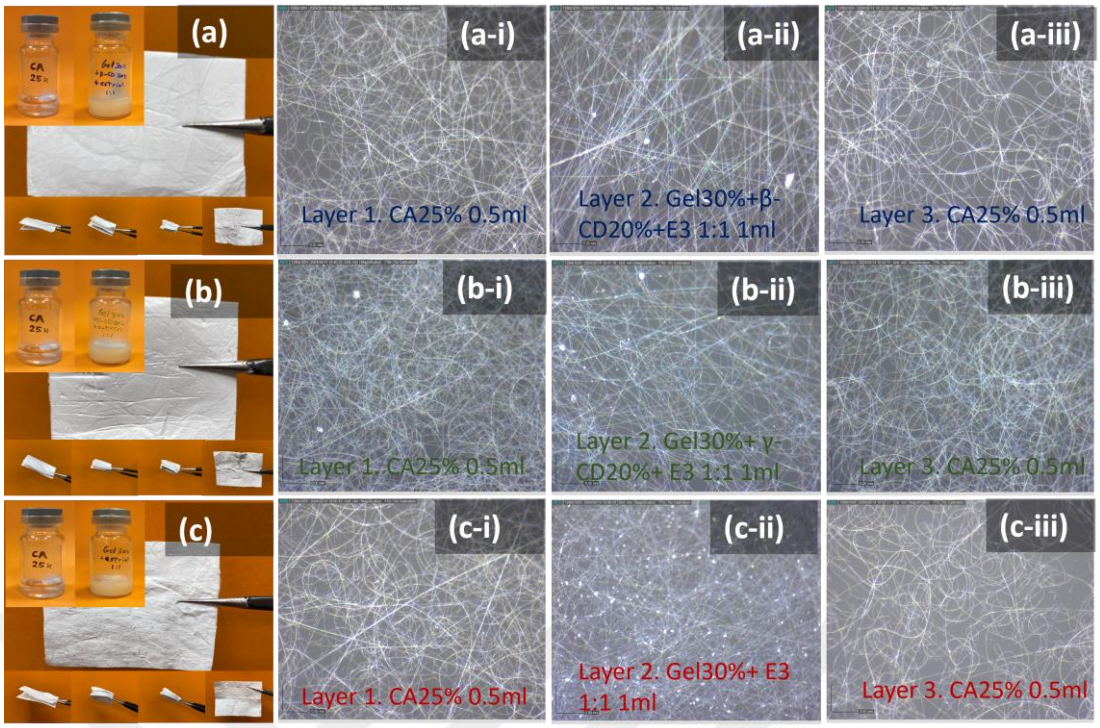

Figure 4.35: Optical images of electrospinning solutions, electrospun nanofibers, and microscopic views of CA+Gel/E3+CA systems with (a) HP-β-CD IC, (b) HP-γ-CD IC, and (c) CD-free formulations at a 1:1 stoichiometric ratio. (i) First layer, (ii) second layer, and (iii) third layer.

The FTIR spectra illustrate the successful incorporation of E3 into a multilayered fiber system composed of CA and Gel layers, both with and without CD ICs (Figure 4.36). The pure E3 spectrum exhibits its characteristic peaks, with distinct C-H stretching around 3000 cm^{-1}, C-H bending, and C-O stretching peaks clearly marked in the fingerprint region. The CDs (HP-β-CD and HP-γ-CD) show their typical broad hydroxyl bands around 3400 cm^{-1} and characteristic peaks in the lower frequency region. CA displays its distinctive peaks that are maintained in the composite structures, while the Gel spectrum demonstrates its characteristic amide bands. In the final multilayered structures (E3/CA/Gel and E3/HP-CD/CA/Gel), the spectra show features from all components, with notable modifications in peak intensities. The presence of CDs in the E3/HP-β-CD/CA/Gel and E3/HP-γ-CD/CA/Gel samples influences the overall spectral profile, indicating successful IC formation within the multilayered fiber structure. These spectral changes provide strong evidence for the successful integration of E3, either directly or as CD complexes, into the CA-Gel multilayered fiber system while maintaining the structural integrity of each component.

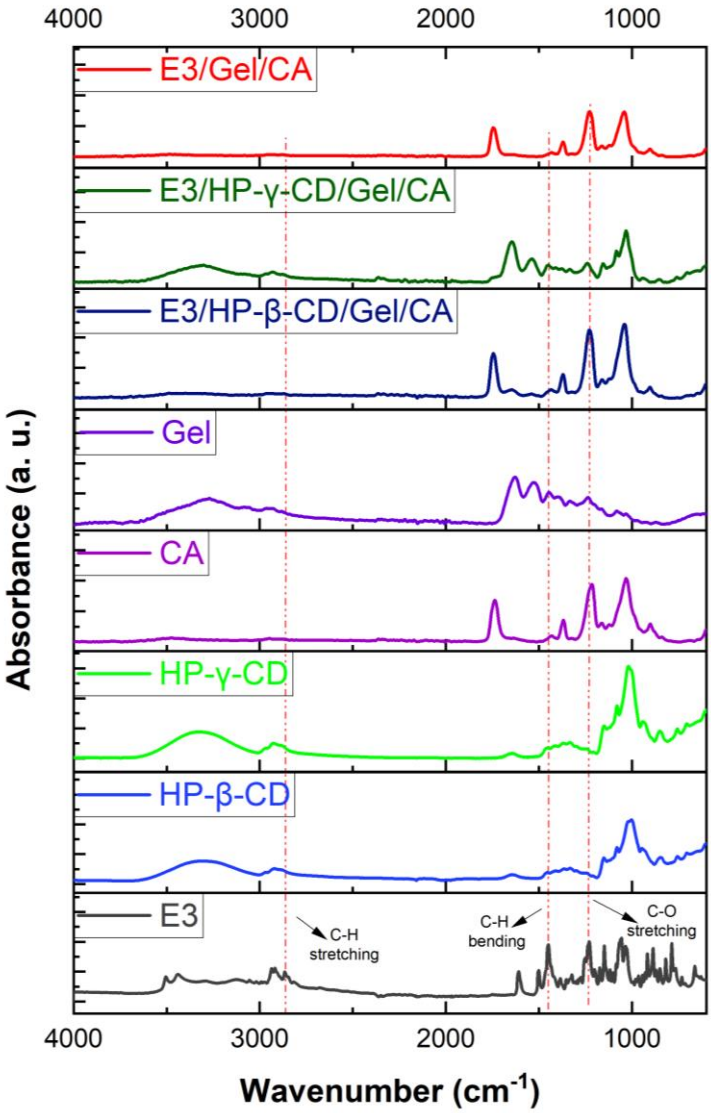

Figure 4.36: FTIR spectra presented from bottom to top: E3, HP-β-CD, HP-γ-CD, CA, Gel, E3/HP-β-CD-Loaded CA-Gel-CA NFs, E3/HP-γ-CD-loaded CA-Gel-CA NFs, and E3-loaded CA-Gel-CA NFs at a (1:1 - E2:CD molar ratio).

TGA analysis of E3 showed that the hormone began to decompose around 200°C, similar to P4 and E2 (Figure 4.37). However, detecting thermal changes for E3 was challenging, as no significant mass loss was observed around 200°C due to its thermal decomposition. This lack of observable change may be attributed to the lower E3 content in the sandwich fiber composition, where the majority of the mass was comprised of CA and Gel.

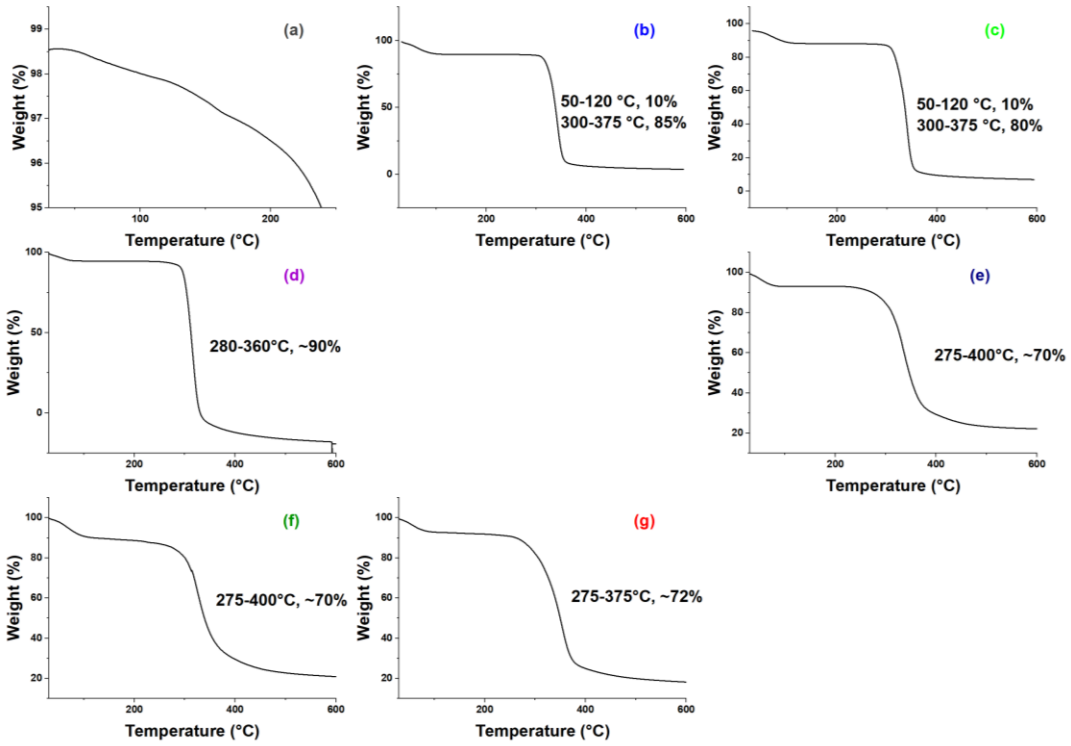

Figure 4.37: The thermogravimetric analysis of (a) E3, (b) HP-β-CD, (c) HP-γ-CD, (d) CA, (e) Gel, (f) E3/HP-β-CD-loaded CA/Gel/CA tri-layered NFs, (f) E3/HP-γ-CD-loaded CA/Gel/CA 3 layered NFs, and (g) E3-loaded CA/Gel/CA 3 layered NFs at a (1:1 - E3:CD molar ratio).

Dissolution testing of the fibers (Figure 4.38) demonstrated that fibers incorporating either type of CD underwent partial dissolution over time, in contrast to the CD-free fibers, which remained intact even after 15 minutes. A similar pattern was observed in dissolution tests performed on tissues pre-wetted with simulated saliva, where sandwich fibers containing HP-β-CD and HP-γ-CD showed partial dissolution, whereas the CD-free sandwich fibers remained undissolved (Figure 4.38).

The release of E3 from the sandwich fibers was monitored over time to assess the influence of cyclodextrin inclusion on the drug's release profile. Higher drug release was observed with the use of CD molecules, indicating that the inclusion complexes formed with HP-β-CD and HP-γ-CD facilitated enhanced drug solubility and diffusion from the fiber matrix. Faster drug release was observed from the fibers containing HP-γ-CD compared to HP-β-CD fibers (Figure 4.39), which may be attributed to the different binding affinities and cavity sizes of the two cyclodextrins. HP-γ-CD, with its larger cavity size, likely accommodates E3 more readily, leading to a quicker dissociation and subsequent release.

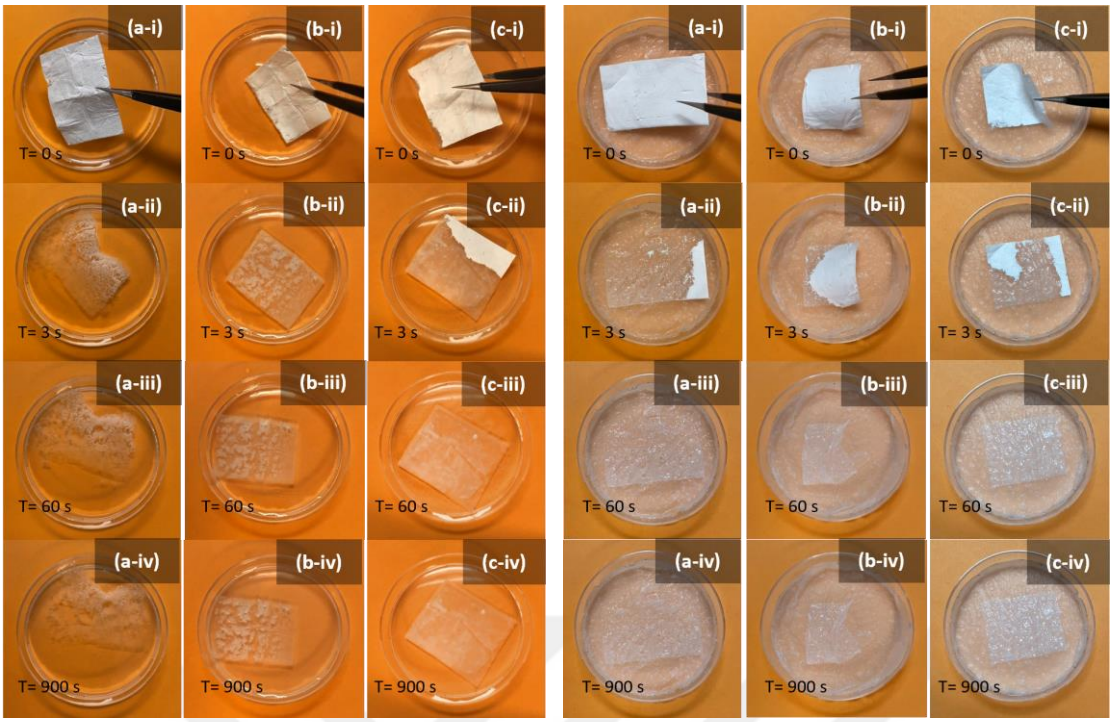

Figure 4.38: (Left panel) The progressive dissolution behavior of tri-layered electrospun mats comprising of CA as outer layers and Gel/E3 incorporated with (a) HP-β-CD, (b) HP-γ-CD and (c) CD-free at 1:1 stoichiometry as the inner layer, in simulated saliva over time. (Right panel) The progressive dissolution behavior of tri-layered electrospun mats comprising of CA as outer layers and Gel/E3 incorporated with (a) HP-β-CD, (b) HP-γ-CD and (c) CD-free at 1:1 stoichiometry as the inner layer, when placed on simulated saliva-moistened tissues.

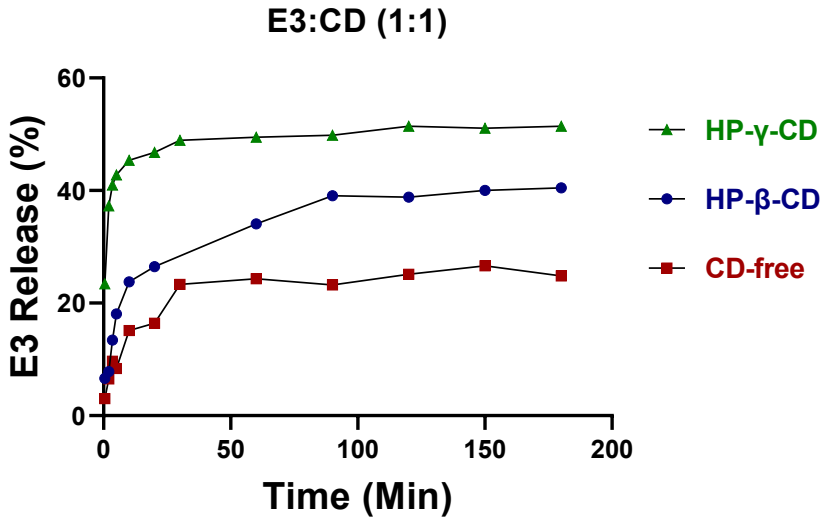

Figure 4.39: Time-dependent in-vitro release profile of tri-layered electrospun mats comprising of CA as outer layers and Gel/E3 incorporated with (a) HP-β-CD, (b) HP-γ-CD and (c) CD-free at 1:1 stoichiometry as the inner layer.

5. CONCLUSIONS

CD-functionalized polymer fibers were fabricated as innovative systems for the rapid and sustained delivery of hormones, with potential for oral administration, particularly for sublingual and buccal delivery. Hormones including P4, E2, and E3 were solubilized using HP-CD molecules through inclusion complexation. The resulting hormone/CD ICs were blended with polymer solutions and electrospun to produce hormone-loaded fibers. CDs played a critical role as solubilizers, enhancing the aqueous solubility of the hormones without the need for toxic organic solvents. It is also utilized to induce drug amorphization within the fiber matrix, enhancing both stability and performance.

Blending the hormone/CD ICs with Pul, a water-soluble polymer, resulted in fast-dissolving fibers. Hormones were loaded at different molar ratios (0.5:1 and 1:1 (hormone:CD)), and the resulting electrospun mats demonstrated flexibility, capable of being folded repeatedly without any rupture, underscoring their potential for commercial use. To assess the impact of CDs, fibers were also fabricated using only drugs, excluding CDs. Comparative studies revealed that CD-containing fibers exhibited both higher drug loading efficiency and faster drug delivery, attributed to the hydrophilic properties of CDs. Structural analysis using optical microscopy and SEM confirmed the formation of bead-free fibers across all hormone formulations. In general, higher hormone content led to thicker fibers due to increased viscosity, while the addition of CDs further contributed to fiber thickening by enhancing solution viscosity. FTIR spectroscopy confirmed the presence of hormones within the fibers through characteristic hormone peaks. Thermal analysis demonstrated improved thermal stability of the hormones, facilitated by inclusion complexation and embedding in the fibers. The fibers were designed to disintegrate rapidly in simulated saliva, dissolving easily on tissues moistened with the same solution. Drug release studies revealed an initial burst release, followed by a sustained release phase. For pullulan fibers, equilibrium in drug delivery was achieved within 30 min, regardless of the hormone type. These findings highlight the potential of CD-functionalized

electrospun fibers as effective, flexible, and scalable systems for oral hormone delivery.

To achieve enhanced control over the delivery of P4, E2 and E3, they were encapsulated within Gel fibers and sandwiched between electrospun CA fibers. CA, a hydrophobic polymer, was utilized to provide a more sustained release of hormones. Like the hormone-loaded Pul fibers, the hormones were incorporated into the Gel fibers using ICs with CD molecules (both HP-β-CD and HP-γ-CD) at 0:5:1 and 1:1 molar ratios. Control fibers were also fabricated without CDs but with equivalent hormone amounts. The resulting multilayered sandwich fibers were flexible and could be folded repeatedly without cracking, demonstrating durability. Microscopic analyses revealed a fibrous structure with occasional bead formations, and all fibers exhibited nanoscale thickness. The successful encapsulation of hormones within the fibers was confirmed by FTIR spectroscopy. Thermal analysis demonstrated improved thermal stability of hormones when embedded in the fibers. Unlike Pul fibers, the CA-based sandwich fibers did not dissolve in simulated saliva or on tissues wetted with saliva due to the hydrophobic nature of CA, allowing for a more prolonged release profile. Importantly, the use of CD molecules (HP-β-CD and HP-γ-CD) not only enhanced the release of the hormones but also increased the overall drug content available for delivery. These findings highlight the potential of multilayered CA-Gel fibers as a robust platform for controlled and sustained hormone delivery.

In the future, the cytocompatibility of the hormone-loaded fibers could be evaluated, as these fibers are designed for oral hormone administration. Additionally, *in vivo* studies could be conducted to measure hormone levels in the blood of mice, providing insights into the bioavailability and systemic absorption of the hormones. Investigating the pharmacokinetics and pharmacodynamics of the fibers in animal models would provide valuable insights into their systemic absorption and therapeutic efficacy. Long-term stability studies under varying storage conditions could establish the shelf life of the fibers, while exploring customizable fiber compositions could allow for tailored hormone doses and release profiles to meet individual patient needs.

REFERENCES

Agnes, M., Pancani, E., Malanga, M., Fenyvesi, E., & Manet, I. (2022). Implementation of Water-Soluble Cyclodextrin-Based Polymers in Biomedical Applications: How Far Are We? *Macromolecular Bioscience*, *22*(8), 2200090. https://doi.org/10.1002/mabi.202200090

Ahmed, F. E., Lalia, B. S., & Hashaikeh, R. (2015). A review on electrospinning for membrane fabrication: Challenges and applications. *Desalination*, *356*, 15-30. https://doi.org/10.1016/j.desal.2014.09.033

Al-Abduljabbar, A., & Farooq, I. (2023). Electrospun Polymer Nanofibers: Processing, Properties, and Applications. *Polymers*, *15*(1), Article 1. https://doi.org/10.3390/polym15010065

Albers, E., & Müller, B. W. (1992). Complexation of steroid hormones with cyclodextrin derivatives: Substituent effects of the guest molecule on solubility and stability in aqueous solution. *Journal of Pharmaceutical Sciences*, *81*(8), 756-761. https://doi.org/10.1002/jps.2600810808

Almousained, M. M., Alshehri, A. A., Aodah, A. H., Alhindi, Y. M., Alqahtani, S. H., Alfassam, H. A., Almomen, A., & Tawfik, E. A. (2024). Development of progesterone electrospun nanofibers to coat Arabin pessaries as a dual preventive and therapeutic approach for preterm labor. *Saudi Pharmaceutical Journal : SPJ*, *32*(2), 101929. https://doi.org/10.1016/j.jsps.2023.101929

Altan, A., Aytac, Z., & Uyar, T. (2018). Carvacrol loaded electrospun fibrous films from zein and poly(lactic acid) for active food packaging. *Food Hydrocolloids*, *81*, 48-59. https://doi.org/10.1016/j.foodhyd.2018.02.028

Araj, S. K., & Szeleszczuk, Ł. (2023). A Review on Cyclodextrins/Estrogens Inclusion Complexes. *International Journal of Molecular Sciences*, *24*(10), Article 10. https://doi.org/10.3390/ijms24108780

Asgari, S., Pourjavadi, A., Setayeshmehr, M., Boisen, A., & Ajalloueian, F. (2021). Encapsulation of Drug-Loaded Graphene Oxide-Based Nanocarrier into Electrospun Pullulan Nanofibers for Potential Local Chemotherapy of Breast Cancer. *Macromolecular Chemistry and Physics*, *222*(15), 2100096. https://doi.org/10.1002/macp.202100096

Aubead, N. M. (2021). Role of Sex Hormones in Human Body. Içinde *Reproductive Hormones*. IntechOpen. https://doi.org/10.5772/intechopen.95778

Aytac, Z., Sen, H. S., Durgun, E., & Uyar, T. (2015). Sulfisoxazole/cyclodextrin inclusion complex incorporated in electrospun hydroxypropyl cellulose nanofibers as drug delivery system. *Colloids and Surfaces B: Biointerfaces*, *128*, 331-338. https://doi.org/10.1016/j.colsurfb.2015.02.019

Balgis, R., Murata, H., Ogi, T., Kobayashi, M., & Bao, L. (2018). Enhanced Aerosol Particle Filtration Efficiency of Nonwoven Porous Cellulose Triacetate Nanofiber Mats. *ACS Omega*, *3*(7), 8271-8277. https://doi.org/10.1021/acsomega.8b00695

Benoit, J. P., Courteille, F., & Thies, C. (1986). A physicochemical study of the morphology of progesterone-loaded poly (d,l-lactide) microspheres. *International Journal of Pharmaceutics*, *29*(2), 95-102. https://doi.org/10.1016/0378-5173(86)90106-7

Bhardwaj, N., & Kundu, S. C. (2010). Electrospinning: A fascinating fiber fabrication technique. *Biotechnology Advances*, *28*(3), 325-347. https://doi.org/10.1016/j.biotechadv.2010.01.004

Blakney, A. K., Ball, C., Krogstad, E. A., & Woodrow, K. A. (2013). Electrospun fibers for vaginal anti-HIV drug delivery. *Antiviral Research*, *100*, S9-S16. https://doi.org/10.1016/j.antiviral.2013.09.022

Bottino, M. C. (2016). Nanofibers for Regenerative Dentistry: From Scaffolds to Drug Delivery Systems. *Microscopy and Microanalysis*, *22*(S3), 996-997. https://doi.org/10.1017/S1431927616005821

Celebioglu, A., & Uyar, T. (2021). Electrohydrodynamic encapsulation of eugenol-cyclodextrin complexes in pullulan nanofibers. *Food Hydrocolloids*, *111*, 106264. https://doi.org/10.1016/j.foodhyd.2020.106264

Coltelli, M.-B., Danti, S., De Clerck, K., Lazzeri, A., & Morganti, P. (2020). Pullulan for Advanced Sustainable Body- and Skin-Contact Applications. *Journal of Functional Biomaterials*, *11*(1), Article 1. https://doi.org/10.3390/jfb11010020

Committee Opinion No. 556: Postmenopausal Estrogen Therapy: Route of Administration and Risk of Venous Thromboembolism. (2013). *Obstetrics & Gynecology*, *121*(4), 887. https://doi.org/10.1097/01.AOG.0000428645.90795.d9

Deitzel, J. M., Kleinmeyer, J., Harris, D., & Beck Tan, N. C. (2001). The effect of processing variables on the morphology of electrospun nanofibers and textiles. *Polymer*, *42*(1), 261-272. https://doi.org/10.1016/S0032-3861(00)00250-0

do Nascimento Soares, G. O., Ribeiro Lima Machado, R., Mendonça Diniz, M., & da Silva, A. B. (2020). Electrospun progesterone-loaded cellulose acetate nanofibers and their drug sustained-release profiles. *Polymer Engineering & Science*, *60*(12), 3231-3243. https://doi.org/10.1002/pen.25549

Ertan, K., Celebioglu, A., Chowdhury, R., Sumnu, G., Sahin, S., Altier, C., & Uyar, T. (2023). Carvacrol/cyclodextrin inclusion complex loaded gelatin/pullulan nanofibers for active food packaging applications. *Food Hydrocolloids*, *142*, 108864. https://doi.org/10.1016/j.foodhyd.2023.108864

Franklin, H. (2020). Progestogens as a component of menopausal hormone therapy: The right molecule makes the difference. *Drugs in Context*. https://dic-wp.zaphod.dev/progestogens-as-a-component-of-menopausal-hormone-therapy-the-right-molecule-makes-the-difference/

Goodman, M. P. (2012). Are all estrogens created equal? A review of oral vs. transdermal therapy. *Journal of Women's Health (2002)*, *21*(2), 161-169. https://doi.org/10.1089/jwh.2011.2839

Grenha, A., & Rodrigues, S. (2013). Pullulan-based Nanoparticles: Future Therapeutic Applications in Transmucosal Protein Delivery. *Therapeutic Delivery*, *4*(11), 1339-1341. https://doi.org/10.4155/tde.13.99

Hsiung, E., Celebioglu, A., Chowdhury, R., Kilic, M. E., Durgun, E., Altier, C., & Uyar, T. (2022). Antibacterial nanofibers of pullulan/tetracycline-cyclodextrin inclusion complexes for Fast-Disintegrating oral drug delivery. *Journal of Colloid and Interface Science*, *610*, 321-333. https://doi.org/10.1016/j.jcis.2021.12.013

Hu, X., Liu, S., Zhou, G., Huang, Y., Xie, Z., & Jing, X. (2014). Electrospinning of polymeric nanofibers for drug delivery applications. *Journal of Controlled Release*, *185*, 12-21. https://doi.org/10.1016/j.jconrel.2014.04.018

Uekama, K., Fujinaga, T., Hirayama, F., Otagiri, M., Yamasaki, M., (1982). Inclusion complexations of steroid hormones with cyclodextrins in water and in solid phase. *International Journal of Pharmaceutics*, *10*(1), 1-15. https://doi.org/10.1016/0378-5173(82)90057-6

Khoshnevisan, K., Maleki, H., Samadian, H., Shahsavari, S., Sarrafzadeh, M. H., Larijani, B., Dorkoosh, F. A., Haghpanah, V., & Khorramizadeh, M. R. (2018). Cellulose acetate electrospun nanofibers for drug delivery systems: Applications and recent advances. *Carbohydrate Polymers*, *198*, 131-141. https://doi.org/10.1016/j.carbpol.2018.06.072

Klausner, D. A., & Ryan, K. J. (1964). Estriol Secretion by the Human Term Placenta. *The Journal of Clinical Endocrinology & Metabolism*, *24*(1), 101-104. https://doi.org/10.1210/jcem-24-1-101

Lavanya, M., Jeyakumar, S., Veerappa, V. G., Pushpadhas, H. A., Ramesha, K. P., Kumaresan, A., Manimaran, A., & Eljeeva Emerald, F. M. (2024). Fabrication and characterization of progesterone loaded pullulan nanofibers for controlled release. *Journal of Drug Delivery Science and Technology*, *91*, 105193. https://doi.org/10.1016/j.jddst.2023.105193

Levitz, M., & Young, B. K. (1978). Estrogens in Pregnancy. İçinde P. L. Munson, E. Diczfalusy, J. Glover, & R. E. Olson (Ed.), *Vitamins & Hormones* (C. 35, ss. 109-147). Academic Press. https://doi.org/10.1016/S0083-6729(08)60522-1

Li, Y., Zhu, J., Cheng, H., Li, G., Cho, H., Jiang, M., Gao, Q., & Zhang, X. (2021). Developments of Advanced Electrospinning Techniques: A Critical Review. *Advanced Materials Technologies*, *6*(11), 2100410. https://doi.org/10.1002/admt.202100410

Liao, S., Li, B., Ma, Z., Wei, H., Chan, C., & Ramakrishna, S. (2006). Biomimetic electrospun nanofibers for tissue regeneration. *Biomedical Materials*, *1*(3), R45. https://doi.org/10.1088/1748-6041/1/3/R01

Loftsson, T., Hreinsdóttir, D., & Másson, M. (2005). Evaluation of cyclodextrin solubilization of drugs. *International Journal of Pharmaceutics*, *302*(1), 18-28. https://doi.org/10.1016/j.ijpharm.2005.05.042

Matencio, A., Bisericaru, D. M., Conesa, I., Er-Rahmani, S., Pedrazzo, A. R., López-Nicolás, J. M., & Trotta, F. (2024). Study of progesterone complexation in cyclodextrins and cyclodextrin-based nanosponges as an example of solvent-free complexation. *Journal of Drug Delivery Science and Technology*, *98*, 105893. https://doi.org/10.1016/j.jddst.2024.105893

Mauri, E., Negri, A., Rebellato, E., Masi, M., Perale, G., & Rossi, F. (2018). Hydrogel-Nanoparticles Composite System for Controlled Drug Delivery. *Gels*, *4*(3), Article 3. https://doi.org/10.3390/gels4030074

Mehdi, M., Hussain, S., Gao, B. B., Shah, K. A., Mahar, F. K., Yousif, M., Hussain, S., & Ahmed, F. (2021). Fabrication and characterization of rizatriptan loaded pullulan nanofibers as oral fast-dissolving drug system. *Materials Research Express*, *8*(5), 055404. https://doi.org/10.1088/2053-1591/abff0b

Morais, M. S., Bonfim, D. P. F., Aguiar, M. L., & Oliveira, W. P. (2023). Electrospun Poly (Vinyl Alcohol) Nanofibrous Mat Loaded with Green Propolis Extract, Chitosan and Nystatin as an Innovative Wound Dressing Material. *Journal of Pharmaceutical Innovation*, *18*(2), 704-718. https://doi.org/10.1007/s12247-022-09681-7

Morales, J. O., Fathe, K. R., Brunaugh, A., Ferrati, S., Li, S., Montenegro-Nicolini, M., Mousavikhamene, Z., McConville, J. T., Prausnitz, M. R., & Smyth, H. D. C. (2017). Challenges and Future Prospects for the Delivery of Biologics: Oral Mucosal, Pulmonary, and Transdermal Routes. *The AAPS Journal*, *19*(3), 652-668. https://doi.org/10.1208/s12248-017-0054-z

Morin-Crini, N., Fourmentin, S., Fenyvesi, É., Lichtfouse, E., Torri, G., Fourmentin, M., & Crini, G. (2020). History of Cyclodextrins. Içinde G. Crini, S. Fourmentin, & E. Lichtfouse (Ed.), *The History of Cyclodextrins* (ss. 1-93). Springer International Publishing. https://doi.org/10.1007/978-3-030-49308-0_1

Özen, İ., & Wang, X. (2023). Biomedicine: Electrospun nanofibrous hormonal therapies through skin/tissue—a review. *International Journal of Polymeric Materials and Polymeric Biomaterials*, *72*(1), 21-39. https://doi.org/10.1080/00914037.2021.1985493

Sabir, F., Asad, M. I., Qindeel, M., Afzal, I., Dar, M. J., Shah, K. U., Zeb, A., Khan, G. M., Ahmed, N., & Din, F. (2019). Polymeric nanogels as versatile nanoplatforms for biomedical applications. *Journal of Nanomaterials*, 2019, 1–16. https://doi.org/10.1155/2019/1526186

Raghav, N., Mor, N., Gupta, R. D., Kaur, R., Sharma, M. R., & Arya, P. (2020). Some cetyltrimethylammonium bromide modified polysaccharide supports as sustained release systems for curcumin. *International Journal of Biological Macromolecules*, *154*, 361-370. https://doi.org/10.1016/j.ijbiomac.2020.02.317

Rutledge, G. C., & Fridrikh, S. V. (2007). Formation of fibers by electrospinning. *Advanced Drug Delivery Reviews*, *59*(14), 1384-1391. https://doi.org/10.1016/j.addr.2007.04.020

Sarkar, K., Gomez, C., Zambrano, S., Ramirez, M., de Hoyos, E., Vasquez, H., & Lozano, K. (2010). Electrospinning to Forcespinning™. *Materials Today*, *13*(11), 12-14. https://doi.org/10.1016/S1369-7021(10)70199-1

Singh, R. S., Saini, G. K., & Kennedy, J. F. (2008). Pullulan: Microbial sources, production and applications. *Carbohydrate Polymers*, *73*(4), 515-531. https://doi.org/10.1016/j.carbpol.2008.01.003

Steffi, C., Wang, D., Kong, C. H., Wang, Z., Lim, P. N., Shi, Z., San Thian, E., & Wang, W. (2018). Estradiol-Loaded Poly(ε-caprolactone)/Silk Fibroin Electrospun Microfibers Decrease Osteoclast Activity and Retain Osteoblast Function. *ACS Applied Materials & Interfaces*, *10*(12), 9988-9998. https://doi.org/10.1021/acsami.8b01855

Taraborrelli, S. (2015). Physiology, production and action of progesterone. *Acta Obstetricia et Gynecologica Scandinavica*, *94*(S161), 8-16. https://doi.org/10.1111/aogs.12771

Tatiana Román, J., Alberto Fuenmayor, C., Dominguez, C. M. Z., Clavijo-Grimaldo, D., Acosta, M., Eduardo García-Castañeda, J., Fierro-Medina, R., & Jenny Rivera-Monroy, Z. (2019). Pullulan nanofibers containing the antimicrobial palindromic peptide LfcinB (21–25) Pal obtained via electrospinning. *RSC Advances*, *9*(35), 20432-20438. https://doi.org/10.1039/C9RA03643A

Tofanica, B.-M., Belosinschi, D., & Volf, I. (2022). Gels, Aerogels and Hydrogels: A Challenge for the Cellulose-Based Product Industries. *Gels*, *8*(8), Article 8. https://doi.org/10.3390/gels8080497

Topuz, F., & Uyar, T. (2019). Electrospinning of Cyclodextrin Functional Nanofibers for Drug Delivery Applications. *Pharmaceutics*, *11*(1), Article 1. https://doi.org/10.3390/pharmaceutics11010006

Topuz, F., & Uyar, T. (2024). Recent Advances in Cyclodextrin-Based Nanoscale Drug Delivery Systems. *WIREs Nanomedicine and Nanobiotechnology*, *16*(6), e1995. https://doi.org/10.1002/wnan.1995

Vyas, A., Saraf, S., & Saraf, S. (2008). Cyclodextrin based novel drug delivery systems. *Journal of Inclusion Phenomena and Macrocyclic Chemistry*, *62*(1), 23-42. https://doi.org/10.1007/s10847-008-9456-y

Wetendorf, M., & DeMayo, F. J. (2012). The progesterone receptor regulates implantation, decidualization, and glandular development via a complex paracrine signaling network. *Molecular and Cellular Endocrinology*, *357*(1), 108-118. https://doi.org/10.1016/j.mce.2011.10.028

Wsoo, M. A., Shahir, S., Mohd Bohari, S. P., Nayan, N. H. M., & Razak, S. I. A. (2020). A review on the properties of electrospun cellulose acetate and its application in drug delivery systems: A new perspective. *Carbohydrate Research*, *491*, 107978. https://doi.org/10.1016/j.carres.2020.107978

Xue, J., Wu, T., Dai, Y., & Xia, Y. (2019). Electrospinning and Electrospun Nanofibers: Methods, Materials, and Applications. *Chemical Reviews*, *119*(8), 5298-5415. https://doi.org/10.1021/acs.chemrev.8b00593

Young, S. L. (2013). Oestrogen and progesterone action on endometrium: A translational approach to understanding endometrial receptivity. *Reproductive BioMedicine Online*, *27*(5), 497-505. https://doi.org/10.1016/j.rbmo.2013.06.010

Zamani, M., Prabhakaran, M. P., & Ramakrishna, S. (2013). Advances in drug delivery via electrospun and electrosprayed nanomaterials. *International Journal of Nanomedicine*, *8*(1), 2997-3017. https://doi.org/10.2147/IJN.S43575

Zhao, L., Duan, G., Zhang, G., Yang, H., He, S., & Jiang, S. (2020). Electrospun Functional Materials toward Food Packaging Applications: A Review. *Nanomaterials*, *10*(1), Article 1. https://doi.org/10.3390/nano10010150

CURRICULUM VITAE

Name Surname **:** Mohamad Yamen Ket

EDUCATION

- **B.Sc.** **:** 2016, Aleppo University, Faculty of Science, Department of Applied Chemistry